



Elevated expression of the retrotransposon LINE-1 drives Alzheimer's disease-associated microglial dysfunction

Nainika Roy^{1,2,3} · Imdadul Haq³ · Jason C. Ngo^{1,2,3} · David A. Bennett⁴ · Andrew F. Teich^{2,3,5} · Philip L. De Jager^{1,2,3} · Marta Olah^{2,3} · Falak Sher^{1,2,3}

Received: 19 September 2024 / Revised: 5 November 2024 / Accepted: 15 November 2024
© The Author(s) 2024

Abstract

Aberrant activity of the retrotransposable element long interspersed nuclear element-1 (LINE-1) has been hypothesized to contribute to cellular dysfunction in age-related disorders, including late-onset Alzheimer's disease (LOAD). However, whether LINE-1 is differentially expressed in cell types of the LOAD brain, and whether these changes contribute to disease pathology is largely unknown. Here, we examined patterns of LINE-1 expression across neurons, astrocytes, oligodendrocytes, and microglia in human postmortem prefrontal cortex tissue from LOAD patients and cognitively normal, age-matched controls. We report elevated immunoreactivity of the open reading frame 1 protein (ORF1p) encoded by LINE-1 in microglia from LOAD patients and find that this immunoreactivity correlates positively with disease-associated microglial morphology. In human iPSC-derived microglia (iMG), we found that CRISPR-mediated transcriptional activation of LINE-1 drives changes in microglial morphology and cytokine secretion and impairs the phagocytosis of amyloid beta (A β). We also find LINE-1 upregulation in iMG induces transcriptomic changes genes associated with antigen presentation and lipid metabolism as well as impacting the expression of many AD-relevant genes. Our data posit that heightened LINE-1 expression may trigger microglial dysregulation in LOAD and that these changes may contribute to disease pathogenesis, suggesting a central role for LINE-1 activity in human LOAD.

Keywords Alzheimer's disease · Microglia · Transposable elements · Retrotransposons · LINE-1 · Neuroinflammation

Introduction

Alzheimer's disease (AD), especially its late-onset form (LOAD), is a complex neurodegenerative disease characterized by cognitive decline and significant neuronal loss.

The pathogenic hallmarks of LOAD encompass a combination of genetic predispositions, environmental factors, and pathological processes including the formation of amyloid-beta (A β) plaques, tau protein hyperphosphorylation, and neuroinflammation [45, 110, 139]. Notably, the presence of sustained neuroinflammation has recently emerged as a key contributing factor in pathological mechanisms of AD [1, 47, 65, 81, 127]. Microglia, the resident immune cells of the brain play a central role in the neuroinflammatory response observed in AD. These cells perform various critical roles in the brain, including maintenance of homeostasis and phagocytosis of cellular debris and pathogens. Strikingly, a majority of AD susceptibility genes discovered through genome-wide association studies are selectively expressed in microglia, and recent studies have identified several AD-linked microglial subpopulations enriched for these risk genes [111, 123, 130, 131].

The strongest known risk factor for AD is aging [40, 108]. Interestingly, aged microglia exhibit shortened processes with altered phagocytosis and immune response,

✉ Falak Sher
fs2644@cumc.columbia.edu

- ¹ Center for Translational and Computational Neuroimmunology, Columbia University Medical Center, New York, NY, USA
- ² Taub Institute for Research On Alzheimer's Disease and Aging Brain, Columbia University Medical Center, New York, NY, USA
- ³ Department of Neurology, Columbia University Medical Center, New York, NY, USA
- ⁴ Rush Alzheimer's Disease Center, Rush University Medical Center, Chicago, IL, USA
- ⁵ Department of Pathology and Cell Biology, Columbia University Medical Center, New York, NY, USA

reduced motility, vacuolization, and large somas [20, 32, 37, 49, 57, 72, 91, 112, 114, 137]. Recently, transposable elements (TEs), formerly regarded as 'junk' DNA, have been recognized for their role in aging-related cellular changes in the brain [36]. TEs are mobile genetic elements capable of changing their genomic locations within human genome through DNA or RNA intermediates [11, 48, 53]. While 45% of the human genome consists of TE-derived repetitive sequences, most have lost their mobility through various genetic and epigenetic modifications [63]. However, aging and pathological conditions can trigger TE derepression, which can induce DNA damage, genomic instability, altered gene expression, and neuroinflammation: features all linked to neurodegeneration [12, 36, 42, 52, 109, 116]. The most abundant and only autonomously mobilizing TE family in humans is the retrotransposon long interspersed nuclear element-1 (LINE-1), which comprises about 17% of the genome [63]. Although majority of the LINE-1s are inactivated due to 5' truncations and the accumulation of inactivating indels, full-length LINE-1 transposition can occur through the transcription of a full-length genomic LINE-1 using the host RNA polymerase II. The resulting bicistronic LINE-1 messenger RNA (mRNA) is exported to the cytoplasm, where it undergoes translation into an RNA chaperone (ORF1p), and an endonuclease and reverse transcriptase (ORF2p). Both ORF1p and ORF2p are essential for LINE-1 transposition [36].

Due to their abundance and repetitive nature, standard quantitative polymerase chain reaction (qPCR) and short-read RNA sequencing (RNA-seq) approaches have limited utility in studying LINE-1 activity [62]. Notably, both bulk and single-cell RNA-seq often cannot distinguish LINE-1 transcripts from bystander transcripts arising from readthrough transcription. Nonetheless, despite these technical challenges, the potential role of LINE-1 activity in neurons and the nervous system has gained attention in recent years [4, 5, 27, 33, 76, 124]. However, its impact on microglia, particularly in the context of AD, remains largely unexplored. We hypothesize that age-associated LINE-1 hyperactivity maybe a driving force behind microglial dysfunction in LOAD.

Pursuing this hypothesis, we investigated the activity of LINE-1 in various brain cells, including neurons, astrocytes, oligodendrocytes, and microglia, using ORF1p expression as an indicator of LINE-1 activity. Analyzing human postmortem prefrontal cortex samples, we found that LOAD patient microglia exhibit heightened LINE-1 activity compared to age-matched controls, with LINE-1 expression correlating with disease-associated microglial morphology. Utilizing CRISPR-mediated transcriptional activation of LINE-1 in human iPSC-derived microglia (iMG), we observed changes in morphology, cytokine production, transcriptomic state, and phagocytic function that

is likely to be relevant for LOAD pathogenesis. Together, these results demonstrate that heightened LINE-1 activity modifies microglial functions, suggesting a potential role of TEs in neurodegeneration.

Materials and methods

Postmortem brain tissue acquisition

Human DL-PFC autopsy tissue sections were from donors in the Religious Orders Study or Rush Memory and Aging Project (ROSMAP) at the Rush Alzheimer's Disease Center (RADDC) in Chicago [6, 7]. Both studies were approved by an Institutional Review Board of Rush University Medical Center and all participants signed informed and repository consents and an Anatomic Gift Act. Additional samples came from Columbia University Medical Center/New York Brain Bank in New York, NY [126]. All samples were acquired with adherence to informed consent protocols. All appropriate approvals were obtained for research procedures from the Institutional Review Board (IRB) of Columbia University Medical Center (protocol AAAR4962). Detailed information regarding donor age, sex, clinical diagnosis, and neuropathology is available in Supplementary Table 1.

Immunohistochemistry (IHC) of postmortem human brain tissue

Tissue sections were deparaffinized using CitriSolv (Decon Labs Inc. Cat. No. 5989-27-5) and rehydrated through progressively decreasing concentrations of ethanol. Microwave antigen retrieval was conducted for 25 min, 30% power using EDTA solution (Sigma-Aldrich, Cat. No. E1161). Sections were then washed and blocked using 3% BSA one hour at RT, and then incubated overnight with primary antibody at 4 °C. The following day, sections were incubated with secondary antibodies for one hour at RT and then washed. Slides were then treated with Biotium TrueBlack Lipofuscin Quencher for 5 min and then washed and mounted with DAPI (Invitrogen, Cat. No.36931). Stained tissue was imaged with the Olympus BX3 Microscope. CellProfiler software was used to perform image analysis and quantification. Antibody concentrations are available in Supplementary Table 2.

Immunoblotting

Harvested cells and homogenized tissue samples were collected in ice-cold RIPA buffer (Cell Signaling Technology, Cat no. 9806S) with freshly added protein inhibitor cocktail and PMSF at a 1:1000 dilution. Samples were then sonicated for 10 s on/off with 20 amplitudes and vortexed before

being lysed on ice for 1 h. Samples were then centrifuged at 12000 *g* for 5 min at 4 °C. The supernatant was isolated and kept as the protein sample. Protein samples were quantified using the Pierce BCA Protein Assay Kits (Thermo Scientific, Cat. No.23225). Samples were appropriately diluted and mixed with SDS Loading Buffer supplemented with DTT and boiled for 5 min at 95 °C. Samples were loaded into 4–20% Mini-PROTEAN TGX Precast Protein Gels (BioRad, Cat no 4561094) for gel electrophoresis and transferred using the Trans-Blot Turbo Mini 0.2 µm PVDF Transfer Packs (BioRad, Cat no. 1704156) and semi-dry transfer system. PVDF membranes were then blocked for 1 h in a solution of equal parts TBS and Intercept (TBS) Blocking Buffer (LICOR, Cat no. 927–60001) at RT. Blots were then incubated with primary antibodies overnight at 4 °C on a shaker. Blots were then washed and incubated with secondary antibody for 1 h at RT on a shaker. Finally, blots were washed and imaged using the Biorad GelDoc Go gel imaging system. FIJI software was used to quantify protein band densities from blots and analyze data. Antibody concentrations are available in Supplementary Table 2.

Human iPSC and astrocyte cell maintenance

Three biologically independent human episomal lines were sourced from Gibco (Cat No. A18945, derived from CD34 + blood cord progenitor cells, healthy female), ATCC (Cat No. ACS-1024, CD34 + bone marrow cells, healthy male) and from the Columbia Stem Cell Initiative (donation, derived from dermal fibroblasts, healthy male). hiPSCs were cultured in mTeSRTM1 (StemCell Technologies, Cat. No. 85850) media. We utilized a human astrocyte line (LONZA Bioscience, Cat No. CC-2565) which was plated on Poly-L-Lysine (PLL) (Sigma, Cat. No. P4707) coated plates and cultured in ABM basal medium (Lonza, Cat. No. CC-3187). Cells were cultured and maintained in 5% CO₂ in a 37 °C humidified incubator. Cells were passaged every 2–3 days. Cultures were regularly examined for mycoplasma contamination.

Generation of LINE-1 overexpression cell lines using CRISPRa

hiPSCs were transduced with a lentiviral vector encoding dCas9-VP64 along in order to stably integrate the CRISPRa machinery. Following this, dCas9-VP64 hiPSCs were transduced using customizable lentiviral vectors [102] carrying single guide RNA (sgRNA) targeting the LINE-1 promoter and a non-targeting (NT) sgRNA with sequences TGG GAGTGACCCGATTTTCC and GTGTGTGTAGCACCG CGTAA respectfully. Successful activation was confirmed through immunoblotting and quantitative PCR assays.

Differentiation from iPSCs to iMG

Differentiations into iMG lines were performed in adherence to a previously published protocol [46]. Briefly, iPSCs were first differentiated into hematopoietic progenitor cells using the STEMdiff Hematopoietic Kit (StemCell Technologies, Cat. No. 05310). The cells are cultured for 3 days with STEMdiff Hematopoietic supplement A, followed by 9 days of culture with supplement B. The media was replaced every 2 days. Following this, cells were relocated to played coated with PLL (Sigma, Cat. No. P4707-50ML) and cultured for 8 days in astrocyte-conditioned media supplemented with growth factors, freshly added during medium replacement. Floating cells at this stage were collected and transferred to PLL-coated plates and cultured in iMG homeostatic medium supplemented with growth factors, to obtain fully differentiated iMG.

Immunocytochemistry (ICC) and morphological analysis using CellProfiler

Cells were plated in 8 well chamber slides prior to ICC. Cells were fixed and permeabilized in ice-cold methanol for 5 min, washed, and then blocked with 10% normal goat serum for 30 min. Cells were then incubated for 1 h or overnight with primary antibody at 4 °C, washed, and then incubated with secondary antibody for 30 min. Chambers were then removed before slides were mounted with DAPI. Details regarding antibody concentrations are available in Supplementary Table 2. Slides were imaged using the Olympus BX3 Microscope. In order to automatically segment cells and measure cellular morphology we utilized CellProfiler v4.2.1. DAPI-positive nuclei were first classified and masked utilizing the ‘IdentifyPrimaryObjects’ module. Typically, the “Threshold” module was applied to the fluorescence channel for a cell-type specific marker (e.g. IBA1), followed by the “ConvertImageToObjects” module. These objects were then filtered for size to exclude artefacts using the “MeasureObjectSizeShape” and “FilterObjects” modules. The objects were further filtered for those containing nuclei using the “RelateObjects” and “FilterObjects” modules. For cells with processes, like microglia, the “SplitOrMergeObjects” was used to ensure branches were associated with their given cell bodies in each object. Once the cells were defined, we applied the “MeasureObjectIntensity” and “MeasureObjectSizeShape” to extract size and morphology information along with fluorescence intensity measurements in the relevant channels. Downstream analyses primarily utilized the “MeanIntensity”, “IntegratedIntensity”, and “Compactness” features to quantify protein expression levels and classify cell morphologies by branch ramification.

Quantitative real-time PCR (qPCR)

1 million cells were harvested, and RNA extraction was carried out using the RNeasy kits. (QIAGEN, Cat. No. 74104). RNA was then converted to cDNA using the iSCRIPT cDNA Synthesis Kit (Biorad, Cat. No. 1708890). Amplified cDNA was purified using SPRI beads and quantified through Qubit. qPCR was conducted using Fast SYBR Green Master Mix (ThermoFisher Scientific, Cat. No. 4385610) with 1 ng of purified cDNA per 10 μ l reaction. qPCR was performed using Quant Studio 4.0 (Applied Biosystem). A list of primers is provided in the extended supplement.

Cytokine profiling

NT or LINE-1 overexpressing iMG were plated in equivalent numbers in a near-homeostatic media [46] and the supernatant was collected after 12 h. A panel of 34 human cytokines and chemokines were used in a multiplex immunoassay platform (Multiplexing Laser Bead Technology) to measure the cytokine concentrations. To identify differentially secreted cytokines, we performed multiple comparisons testing using the Benjamini–Hochberg procedure to control for the false discovery rate. A q value of 0.01 (1%) was used to determine the significance threshold.

Phagocytosis of A β ₄₂

Phagocytosis assays were performed using 647-fluorescently conjugated A β ₄₂ (ANASPEC, Cat No. AS-64161). For ICC-based phagocytosis experiments, iMG were plated in chamber slides, for flow cytometric experiments, iMG were plated in 12-well plates. In both cases, iMG were incubated with 0.5 μ M A β for 2 h at 37 °C. For ICC-phagocytosis, a fluorescently conjugated actin antibody (ThermoFisher Scientific, Cat No. A57246) was added in the last 30 min to enable cell masking and visualization. In both A β ₄₂ phagocytosis experiments, we included a sample of iMG which was pre-treated with cytochalasin-D [89], an inhibitor of phagocytosis, as an additional control to validate our assay. Cells were then washed three times with PBS. For ICC, chamber slides were removed before slides were mounted with DAPI and imaged using the Olympus BX3 Microscope. Images were analyzed and quantified using CellProfiler software. For flow cytometric phagocytosis, a BD Influx sorter was used for cytometric analysis and FlowJo software was used to visualize and analyze the data.

Bulk RNAseq of iMG

Sequencing

Total RNA was extracted from iMG using RNeasy kits. (QIAGEN, Cat. No. 74104) RNA quality was assessed via

Bioanalyzer (RIN > 9.5). Libraries were prepared using the TruSeq Stranded mRNA Library Prep Kit (Illumina, Cat No. 20020595). Samples underwent 2 \times 75 bp paired-end sequencing on the Aviti Element at the Columbia Genome Center. Above 15 million reads were obtained per sample, and the experiment was performed on three independent biological replicates.

Analysis

Kallisto[10] was used to produce quantification of transcript abundance. The raw counts per gene were analyzed using DESeq2 [34, 71] to identify genes that were significantly differentially expressed between NT and LINE-1⁺ iMG samples. Log fold change > 0.5 and q < 0.01 parameters were used to determine significance thresholds.

For GO analysis, the 100 most significantly upregulated and downregulated DEGs in the LINE-1 + iMG compared to control were examined through Enrichr using the GO Molecular Function 2023 gene set library. Enrichment analysis was also performed on the list of 100 most significantly upregulated DEGs using the Database of Genotypes and Phenotypes (dbGaP) to identify phenotypes related to the transcriptional signature of the LINE-1 + iMG.

Results

LINE-1 activity is found in major CNS cell types of the aged human brain

Endogenous retrotransposition is perhaps best known for driving genetic variation in the germline and in oncogenesis [50, 52], and was previously considered to be largely silenced. However, multiple subsequent reports have documented somatic activation of LINE-1, including in the human brain [5, 24, 26, 27, 54, 82, 87, 124] and in aging [33]. Previous studies examining LINE-1 transposition in the brain have utilized methylation as an indirect readout of activity; whole-genome sequencing, or bulk or single-cell RNA sequencing methodologies have also been used to examine LINE-1 abundance and expression. While these efforts provide valuable insight into LINE-1 dynamics, challenges due to the repetitive and polymorphic nature of LINE-1 insertions restrict their ability to accurately quantify and compare active expression. Conversely, examining the presence of LINE-1 proteins can indicate active transposition occurring during given time period, such as in aging. To date, no study has examined the presence of LINE-1 proteins at a cell-type resolution in the brain.

To begin disentangling the potential role of transposon activity in neurodegenerative disease, we first sought to determine whether LINE-1 activity was found in aged

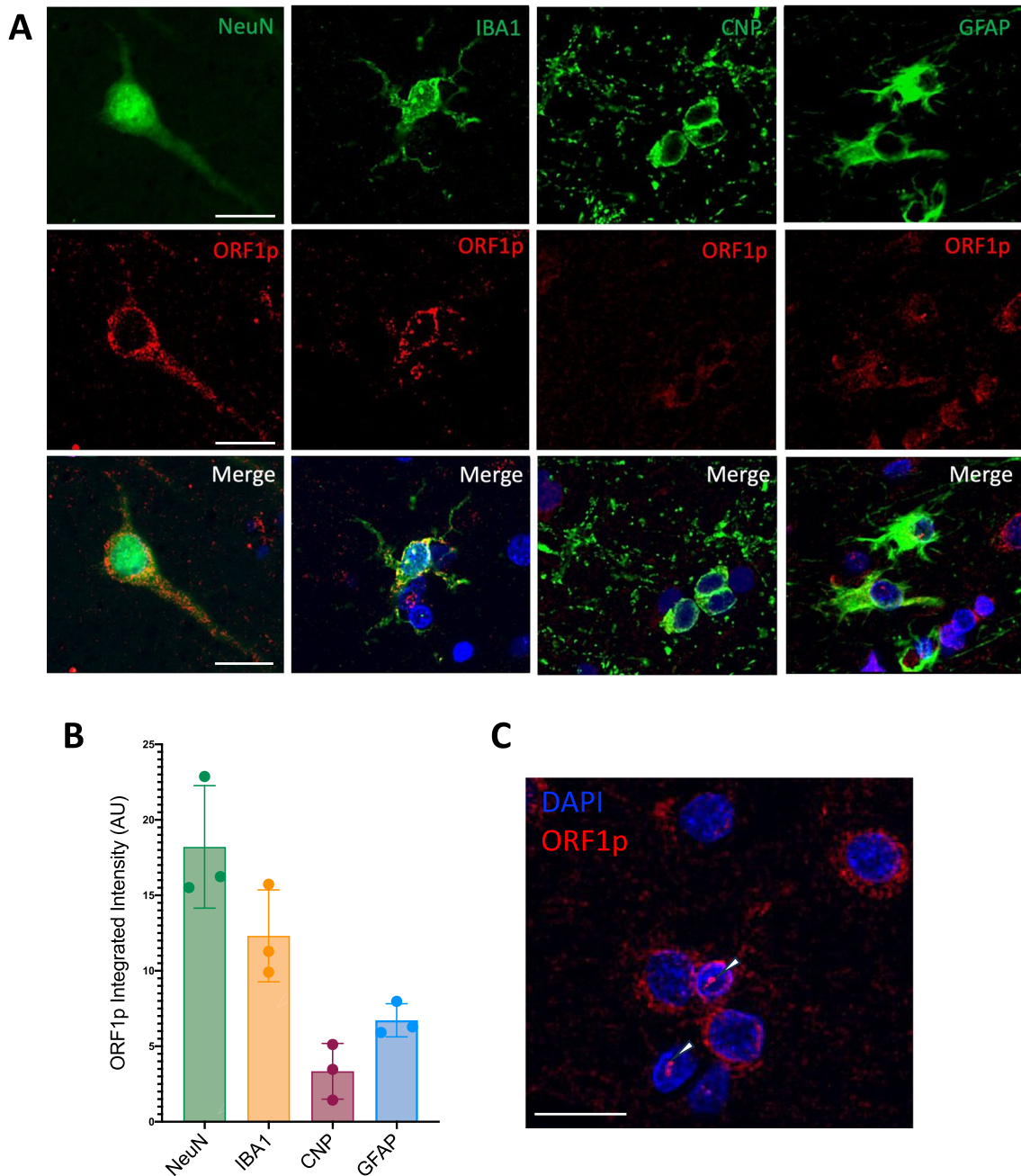
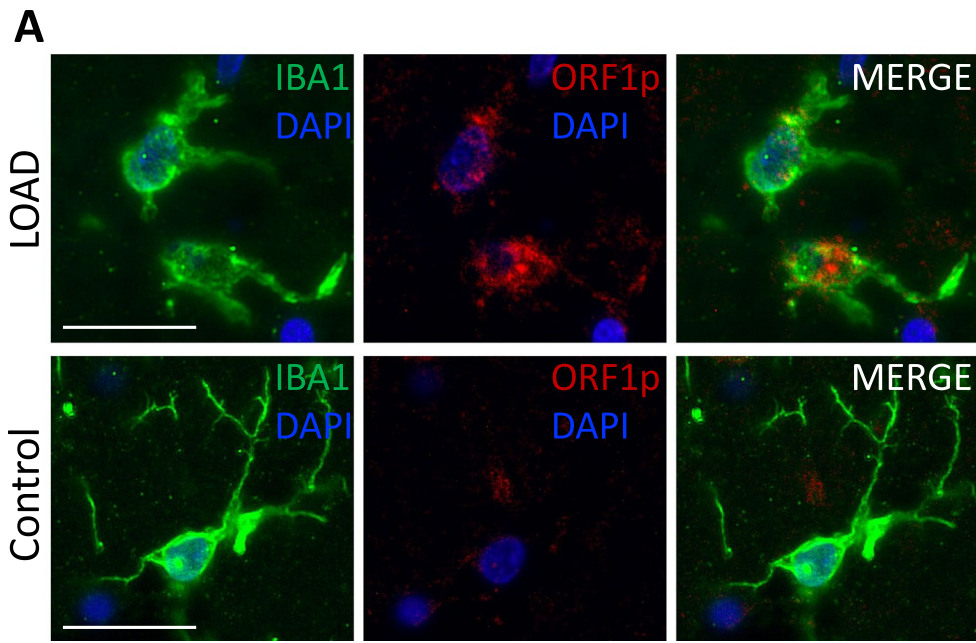


Fig. 1 LINE-1 activity is found in major CNS cell types of the aged human brain. **A** Representative images showing endogenous LINE-1 ORF1 (ORF1p) protein expression in cognitively healthy human DLPFC postmortem brain tissue in NeuN, IBA1, CNP and GFAP positive cells using indirect immunohistochemistry. **B** Quantification of average ORF1p integrated (total) fluorescence intensity/cell from

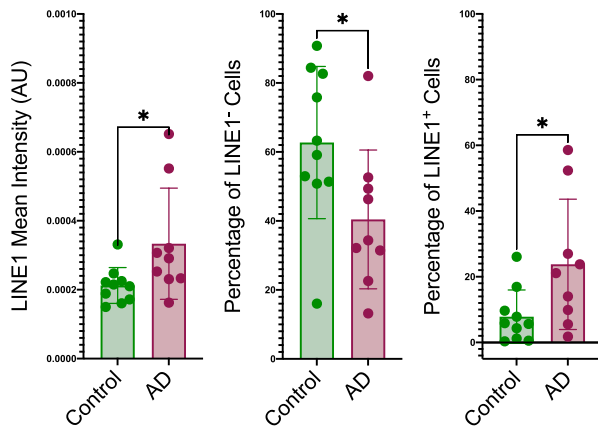
three healthy DLPFC donors. Number of cells analyzed are 5937, 1565, 440 and 62 for NeuN+, IBA1+, CNP+ and GFAP+ cells respectively. **C** A representative image of LINE-1 ORF1p expression in the nucleus. Scale bar represents 10 μ m. Cell type markers are shown in green, ORF1p shown in red and DAPI represented as blue

human brain tissue and across cell types. We used an antibody against LINE-1 ORF1p, a protein encoded by LINE-1 that is produced during retrotransposition, to measure active LINE-1 transcription. We co-immunostained human post-mortem dorsolateral prefrontal cortex (DLPFC) tissue with ORF1p and markers for different cell types in the brain. We

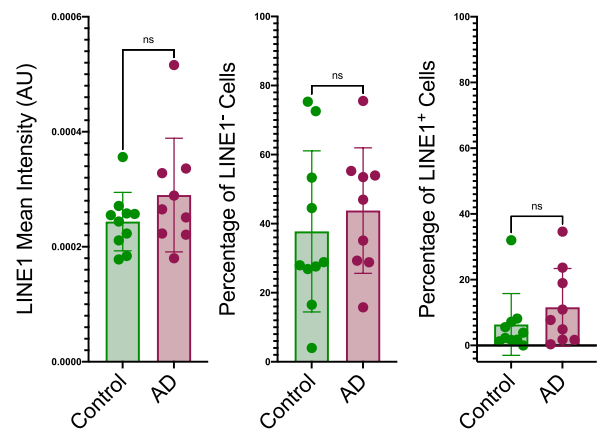
found ORF1p immunoreactivity in neurons, microglia, oligodendrocytes, and astrocytes, labeled by NeuN, IBA1, CNP and GFAP, respectively (Fig. 1a). As expected, we noted the highest ORF1p immunoreactivity in NeuN-positive neurons, as previous studies have reported LINE-1 expression in human neurons and neuronal cell lines [87, 119,



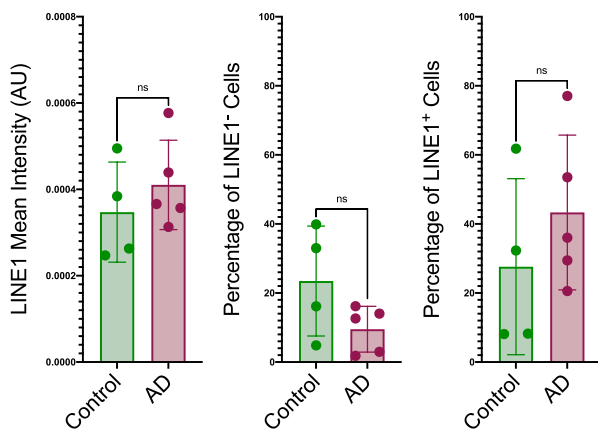
B IBA1+ cells



C NeuN+ cells



D GFAP+ cells



E CNP+ cells

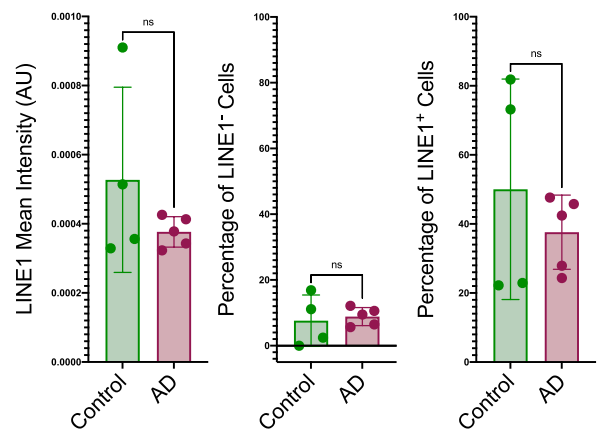


Fig. 2 Microglial LINE-1 ORF1p protein expression is increased in LOAD patients. **A** Representative images of IBA1 (green), ORF1p (red) and DAPI (blue) immunostaining in human postmortem brain tissue from LOAD patients and cognitively healthy controls examined by fluorescence microscopy. Scale bars represent 10 μm . **B–E** Comparison of average LINE-1 ORF1p mean fluorescence per cell (AU) (left), the percentage of ORF1p-low expressing cells (middle) and the percentage of ORF1p-high expressing cells (right) between control and LOAD DLPFC microglia (**B**), neurons (**C**), astrocytes (**D**) and oligodendrocytes (**E**). Experimental information is as follows: **B** IBA1+ cells; $n=9$ (control subjects) and $n=10$ (LOAD subjects); average of 417 cells analyzed per patient. (**C**) NeuN+ cells; $n=9$ (control subjects) and $n=10$ (LOAD subjects); average of 532 cells analyzed per patient. (**D**) GFAP+ cells; $n=4$ (control subjects) and $n=5$ (LOAD subjects); average of 176 cells analyzed per patient. **E** CNP+ cells; $n=4$ (control subjects) and $n=5$ (LOAD subjects); average of 74 cells analyzed per patient. Data are presented as mean \pm S.D. and analyzed using an unpaired two-tailed t test; * $P \leq 0.05$; ns : not significant. Exact P values can be found in source text. A detailed table with information regarding the human subjects and diagnosis can be found in Supplementary Table 1. Further information on image acquisition and analysis can be found in the Methods

124]. Intriguingly, we also observed strong ORF1p staining within IBA1-positive microglia. GFAP-positive astrocytes and CNP-positive oligodendrocytes also exhibited LINE-1 activity, albeit to a lesser extent (Fig. 1b).

While the ORF1p signal was primarily found in the cytoplasm, we detected occasional strong punctate staining in the nucleus, in line with previous reports from various human in vitro cell systems [35, 85, 105, 107] (Fig. 1c). Using an antibody that has been tested multiple times for immunohistochemistry immunoprecipitation, and immunoblotting [23, 99, 118, 132], we detected LINE-1-encoded protein rather than merely identifying LINE-1 sequences. This finding confirms the expression of LINE-1 at the time of autopsy within these aged tissue samples. Together, these data reveal that active LINE-1 translation occurs across multiple cell types of the aged human brain, supporting the compelling hypothesis that LINE-1 may contribute to age-related disorders.

LINE-1 activity is altered in LOAD patients compared to non-AD controls

To examine whether aberrant LINE-1 activity is linked to late-onset AD, we compared LINE-1 ORF1p expression across cell types (Fig. 2a, Supplementary Figure S2) of the brain in late-onset AD patient postmortem tissue from the DLPFC to an older cohort of non-AD controls (Supplementary Table 1). Strikingly, we found a significant increase in LINE-1 ORF1p mean fluorescence in IBA1+ cells in LOAD patients compared with controls ($p=0.0172$) (Fig. 2b, AU). Due to the non-normal distribution in the AD group (Shapiro–Wilk test, $p=0.0414$), we applied the Mann–Whitney U test. The two-tailed analysis revealed a significant difference between the groups ($U=16$, $p=0.0172$), with the

median of the control group at 0.0002125 ($n=10$) and the AD group at 0.0002910 ($n=9$). The difference in medians was $7.850e-005$, with a Hodges–Lehmann estimate of $8.100e-005$, indicating a statistically significant increase in LINE-1 activity in LOAD.

To further explore this difference, we established thresholds for LINE-1 expression based on the upper and lower quartiles of ORF1p fluorescence intensity across all cell types. We found a significantly reduced percentage of cells with low LINE-1 expression in LOAD compared to controls ($p=0.0351$), and a significantly increased percentage of cells with high LINE-1 expression in LOAD ($p=0.0318$) (Fig. 2b, percentage).

While the ORF1p mean fluorescence intensity in NeuN+, GFAP+ and CNP+ cells trended higher in LOAD patients compared to control (Fig. 2c–e), these differences did not reach statistical significance, possibly due to our small sample size. The detection of elevated LINE-1 activity in microglia suggests that microglia may be particularly vulnerable to disease-related epigenomic changes, although this apparent selectivity may be influenced by sample size. Importantly, previous epigenetic studies have shown that DNA methylation signatures enriched in LOAD are largely driven by variation in microglia [21, 106]. These findings emphasize the potential role of LINE-1 activity in LOAD-associated neuropathology.

LINE-1 activity correlates with disease-associated microglial phenotypes in the human brain

We next sought to investigate whether LINE-1 activity patterns in the brain were associated with microglia phenotypes typically associated with LOAD. We first examined whether there was a relationship between LINE-1 activity and microglial morphological state. Microglial morphology is believed to be tightly linked to its function [60, 135]. Under homeostatic conditions, microglia are highly ramified with branched processes required for microenvironment surveillance and motility [90, 97]. Microglia from LOAD brains can present with a morphology marked by de-ramification and reduced arborization [29].

Using CellProfiler, we examined IBA1+ microglia from nine AD-samples (Supplementary Table 1) to quantify their morphology, segregating cells into “Ramified” and “Ameboid” categories based on their degree of branch arborization (see Fig. 3a and Methods section). We found that microglia classified as ameboid had significantly higher mean ORF1p fluorescent intensity than ramified microglia ($p=0.0067$) (Fig. 3b). Similarly, there was a significantly higher percentage of ORF1p-positive cells in the ameboid microglia group than the ramified ($p=0.0093$) (Fig. 3c). When stratified by disease state, we found that LOAD

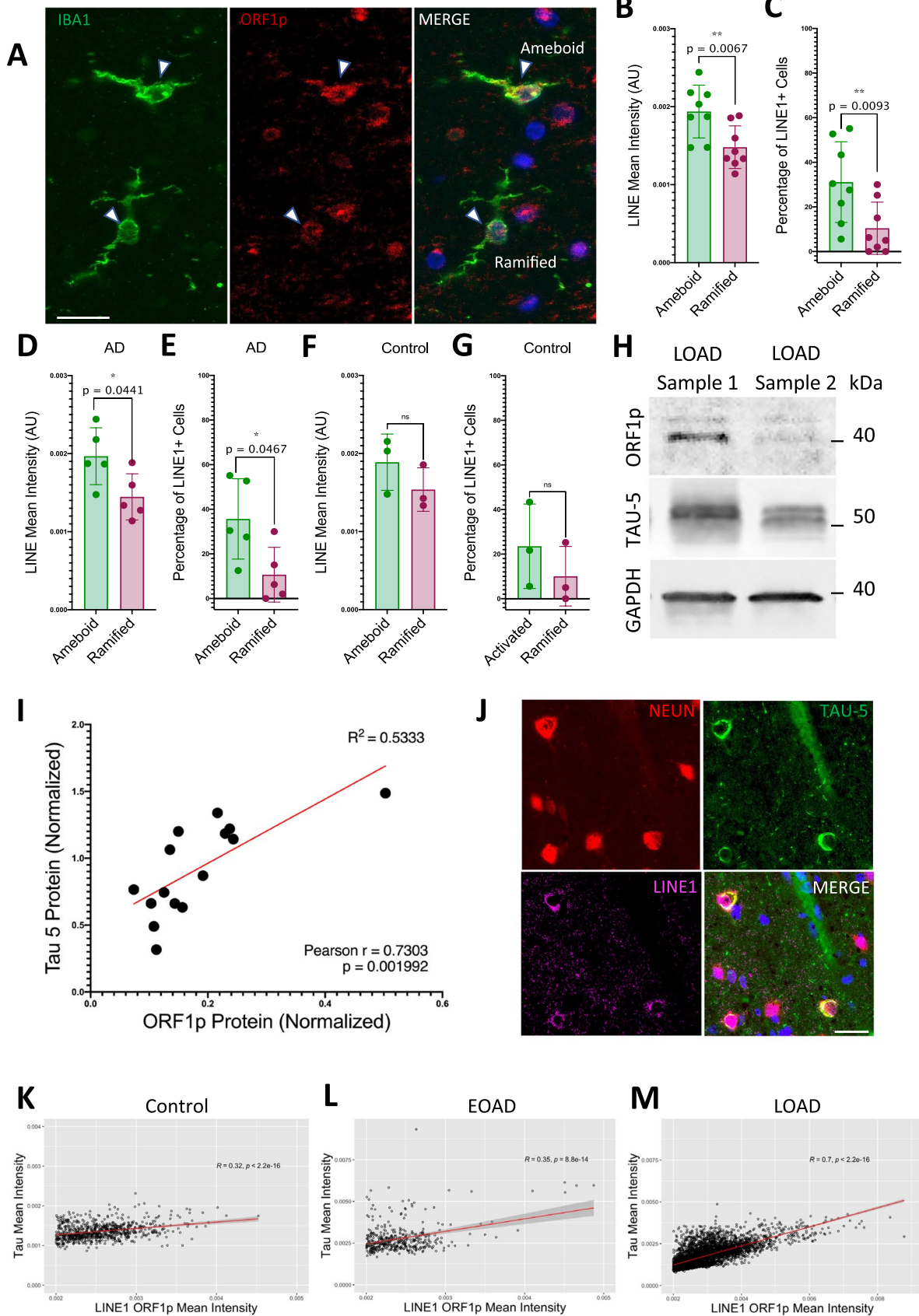


Fig. 3 LINE-1 activity correlates with AD-associated phenotypes in the human brain. **A** Representative images of IBA1 (green), ORF1p (red) and DAPI (blue) immunostaining demonstrating ORF1p expression level correlating with morphology in microglia; example cells denoted by white arrow. Scale bars represent 20 μ m. **B** Comparison of average LINE-1 ORF1p mean fluorescence intensity per cell (AU) in amoeboid and ramified microglia. **C** Comparison of percentage of cells with LINE-1 activity in amoeboid and ramified microglia. **D–G** Data from **B** and **C** stratified by disease state: LOAD (**D** and **E**) and control (**F** and **G**). $n=8$ subjects (5 LOAD and 3 control). An average of 428 microglial cells were analyzed per individual subject. **H** Representative immunoblot and **I** and immunoblot quantification shown on a scatterplot of LINE-1 ORF1p and Tau-5 levels from 5 control and 10 LOAD patients, finding a strong linear correlation (Pearson $r=0.7303$) between LINE-1 ORF1p and Tau-5 protein levels. Image densities were normalized to GAPDH expression prior to examining correlation. **J** Representative immunostaining from LOAD postmortem brain tissue showing strong overlap between LINE-1 ORF1p expression (pink) and Tau expression (green) in NeuN-labeled neurons (red). Scale bars represent 10 μ m. **K–M** Scatter plots demonstrating a modest correlation between Tau and LINE-1 in neurons from control patients, and a strong correlation between Tau and LINE-1 in neurons from EOAD and LOAD patients. $n=2$ control subjects, with an average of 804 neurons analyzed per subject; $n=3$ EOAD subjects, with an average of 358 neurons analyzed per subject; $n=4$ LOAD subjects, with an average of 1358 neurons analyzed per subject. Data in **B–G** are presented as mean \pm S.D. and analyzed using an unpaired two-tailed t test; * $P\leq 0.05$; ** $P\leq 0.01$, ns: not significant. Exact P values can be found in source text. A detailed table with information regarding the human subjects and diagnosis can be found in Supplementary Table 1. Further information on image acquisition and analysis can be found in the Methods

patients exhibited a similar pattern of higher ORF1p intensity ($p=0.0441$) and a greater percentage of ORF1p-positive cells ($p=0.0467$) in the amoeboid population compared to the ramified (Fig. 3d, 3e). We did not find significant differences in LINE-1 activity in our non-AD samples (Fig. 3f, 3g), but it is unclear whether that is due to limited sample size or any sort of disease association. These results suggest that LINE-1 activity is associated with microglial morphology and may contribute to the activated microglial phenotype associated with AD [29].

LINE-1 activity is associated with tau pathological burden in the human brain

One distinguishing feature of AD and other tauopathies is the accumulation of intracellular neurofibrillary tangles, which are comprised of insoluble aggregates of the microtubule-associated protein tau (MAPT) [2, 95]. Intriguingly, tau burden is associated with extensive chromatin remodeling, loss of TE silencing, and its subsequent activation [31, 39, 42, 58, 116]. We investigated whether there was a correlation between LINE-1 activity and tau pathologic burden in aged patient samples. We extracted protein from the DLPFC of 15 postmortem human brains (5 non-AD control and 10 LOAD patients) and immunoblotted for levels of Tau-5 [15, 68], LINE-1 ORF1p and GAPDH. After normalizing sample

proteomic values to GAPDH, we found a strong correlation between LINE-1 ORF1p and Tau 5 protein levels ($r=0.730$, $p=0.002$) (Fig. 3h, 3i).

Since neurons are the primarily cell type with tau pathology, we used immunohistochemistry on patient postmortem tissue to examine the overlap between ORF1p and Tau-5 immunostaining in NeuN+ cells. We found a strong correlation between ORF1p and Tau 5 mean fluorescence intensity in control, LOAD and EOAD cells, with the strongest correlation found in LOAD and similar correlations in EOAD and control (Fig. 3j–m). The differences in the correlation between LOAD and control samples may be explained by the lack of significant tau pathology in the control samples, evidenced by the average and highest tau intensity values being much lower in control samples than in the AD. Interestingly, the correlation in LOAD ($r=0.7$) was stronger than in EOAD ($r=0.35$), despite higher tau intensity levels in EOAD, indicating a potential link between age and retrotransposition activity in AD.

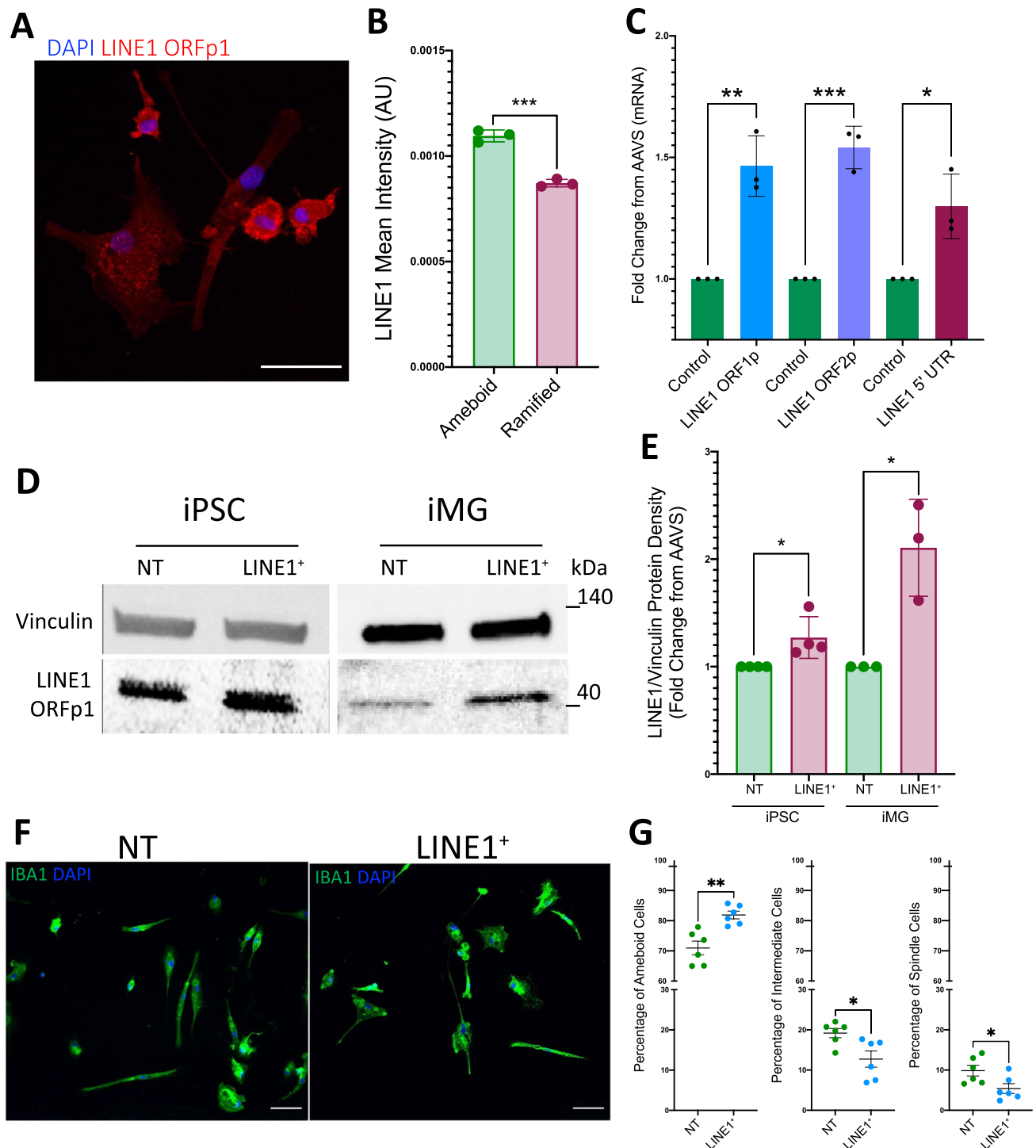
These findings confirms a relationship between neuronal LINE-1 activity and tau burden, further highlighting the role of LINE-1 in AD pathology across multiple brain cell types.

To further explore the relationship between Tau and LINE-1 expression in neurons, we stratified neurons based on low, medium, and high Tau or ORF1p expression (Fig. S3a–f). The positive correlation between ORF1p and Tau was strongest in neurons with low Tau and high ORF1p expression, potentially indicating that Tau's impact on LINE-1 regulation may be most prominent in early stages of Tau pathology. In addition, we compared mean ORF1p expression in non-AD and LOAD neurons within low-Tau and high-Tau subsets (Figure S3g). Although ORF1p expression trended higher in LOAD neurons across both subsets compared to non-AD, the difference was not statistically significant in our small sample size.

Overexpression of LINE-1 induces hyporamification in iMG

Our analysis of LINE-1 expression in postmortem tissue established an association between retrotransposition and microglial morphology but it was not suited to define the directionality of this relationship. We hypothesize that heightened LINE-1 activity in microglia contributes to a shift from a homeostatic state towards morphologically activated state, which is associated with LOAD [20, 104, 115]. To ascertain whether LINE-1 transposition induces these morphological changes in microglia, we turned to an in vitro system where we could manipulate transposition activity: a human pluripotent stem cell-derived microglia model (iMG) previously established in our laboratory [46].

We first examined whether iMG in culture recapitulated the relationship between LINE-1 activity and microglial



morphology. Indeed, immunostaining experiments revealed that ameboid cells within the iMG culture had significantly higher expression of LINE-1 ORF1p than spindle or ramified cells ($p = 0.0003$) (Fig. 4a, 4b). To disentangle the causal direction of the relationship between LINE-1 activity and morphologically active (ameboid) phenotype, we used the CRISPR-activation system (CRISPRa) [59, 103] with single guide RNAs (sgRNAs) targeting putative LINE-1 promoters

to drive increased expression of the LINE-1 gene in human iPSCs that we differentiated into iMG, termed henceforth as LINE-1⁺ iMG. Alongside this, we utilized the same system with reference sgRNAs targeting the sequences not present in human genome, as a control (NT). We established that forced LINE-1 transcriptional activation does not disrupt typical microglial differentiation using qPCR and our previously validated set of microglial markers [46] (Fig. S4a).

Fig. 4 Overexpression of LINE-1 induces hyporamyfication in iMG. **A** Representative fluorescence microscopy image of wild-type iMG ORF1p (red) and DAPI (blue) immunostaining in iMG showing increased expression ameoboid iMG and reduced expression in ramified iMG. Scale bar represents 10 μ M. **B** Comparison of ORF1p immunofluorescence intensity in ameoboid and ramified iMG. $n=3$ (three independent differentiations). An average of 245 iMG were analyzed per iMG line/experiment. **C** Relative mRNA expression of LINE-1 ORF1p, LINE-1 ORF2p and LINE-1 5' UTR is increased in LINE-1⁺ iMG compared to control (NT-iMG). $n=3$ biologically independent experiments. **D** Representative immunoblots and **E** quantifications of LINE-1 ORF1p and Vinculin protein showing increased ORF1p in iPSCs and corresponding iMG overexpressing LINE-1 compared to control (NT-iMG). **F** Representative images of IBA1 (green) and DAPI (blue) immunostaining showing cellular morphology in LINE-1-overexpressing iMG and NT control iMG. Scale bar represents 50 μ m. **G** Quantification of the percentage of cells with ameoboid, intermediate, and ramified morphology of LINE-1-overexpressing or NT control iMG, showing a significant increase of ameoboid cells and a significant decrease in intermediate and ramified cells in LINE-1 overexpressing iMG compared with NT control. $n=6$ experimental replicates, 3 biologically independent samples. An average of 274 iMG were analyzed per experimental replicate. Data are presented as mean \pm S.D. and analyzed using an unpaired two-tailed t test; * $P \leq 0.05$; ** $P \leq 0.01$, *** $P \leq 0.001$, ns: not significant. Exact P-values can be found in source text

We then examined phenotypic changes in LINE-1⁺ iMG compared with our reference NT- iMG. We first confirmed that our system successfully produced increased LINE-1 transcription in the iPSC as well as the differentiated iMG through the detection of significantly elevated ORF1p, ORF2p and 5' UTR mRNA (Fig. 4c) and of ORF1p protein (Fig. 4d, e). We then assessed whether the induction of LINE-1 transcription influenced iMG morphology. Intriguingly, we found that LINE-1⁺ iMG had a significantly higher percentage of ameoboid cells ($p=0.002$) compared with NT iMG, and a significantly lower percentage of intermediate ($p=0.019$) and ramified cells ($p=0.033$) (Fig. 4f, 4g). These data corroborate the correlation between retrotransposon activity and morphological changes in microglia and finds that boosting LINE-1 transcription is sufficient to induce this phenotypic shift.

Increased LINE-1 expression induces an altered cytokine secretion profile in iMG

We next sought to assess whether the morphological changes we observed in LINE-1⁺ iMG also reflected functional alterations. Microglia react to changes in cellular milieu in the brain but also have the ability to influence their microenvironment through cytokine production and signaling. LOAD is associated with a strong upregulation of pro-inflammatory patterns of cytokine secretion, induced by disease-associated stimuli such as A β -plaques [69]. Sustained inflammation drives high production of these cytokines and contributes to cognitive decline [127]. We sought to assess the impact

of increased LINE-1 activity on the cytokine secretion profile of iMG. We utilized multiplex immunoassay platform (Multiplexing Laser Bead Technology), to measure the levels of 34 human cytokines and chemokines secreted into the culture media of LINE-1 + and NT-iMG (Fig. 5a). To account for multiple hypotheses and control for false discoveries, we applied the Benjamini–Hochberg procedure for multiple comparisons testing. A stringent q-value threshold of 0.01 (1% false discovery rate) was set to ensure robust identification of differentially secreted factors. This analysis revealed 9 cytokines that were significantly altered in the LINE-1 + condition compared to NT-iMG: IL-10, RANTES, VEGF-A, IL-1 α , MIP-1 α , MIP-1 β , GM-CSF, CXCL9, and PDGF-AA.

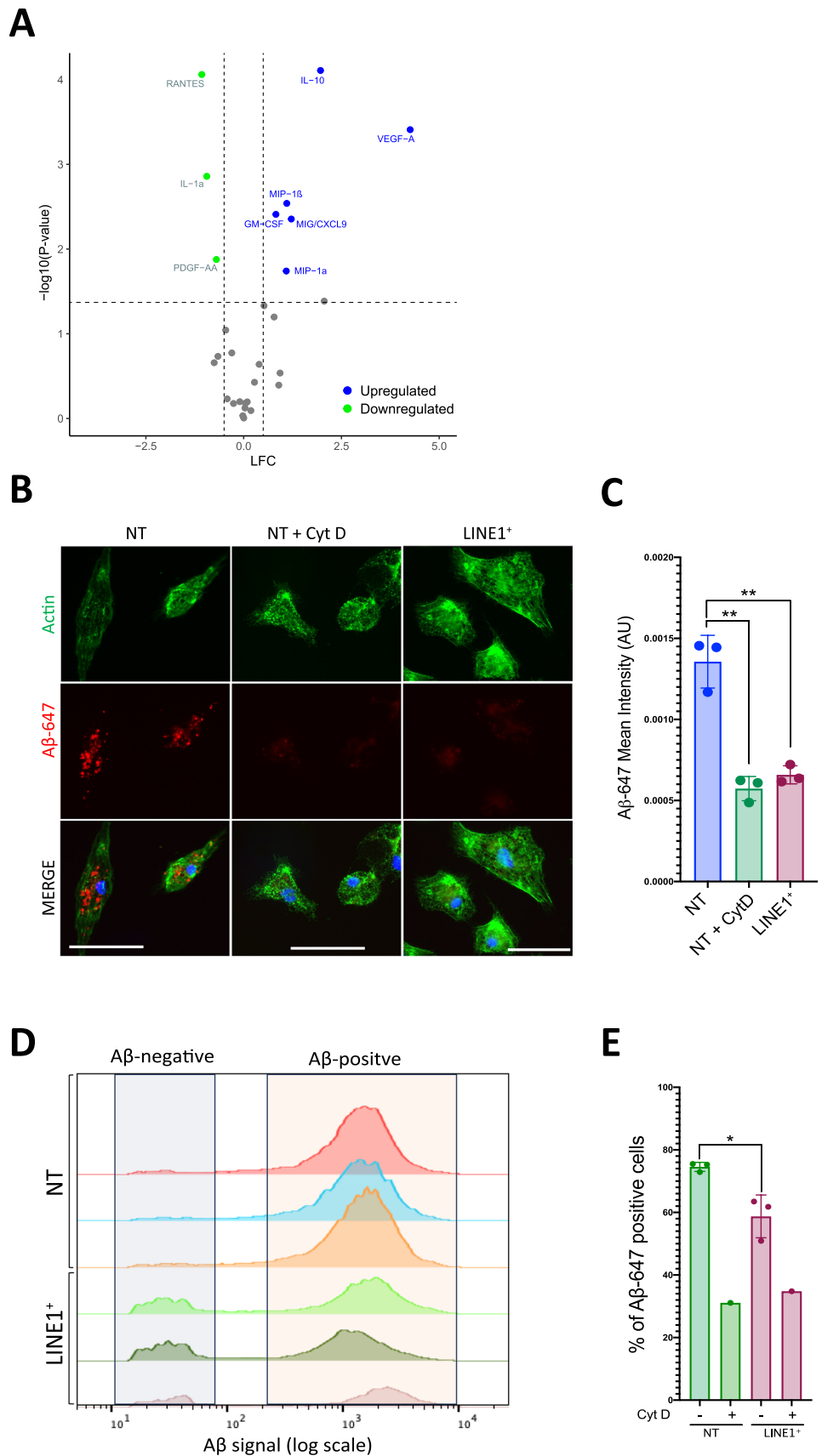
A closer look at these cytokines revealed an interesting altered immune profile of LINE-1⁺ iMG. A majority of these cytokines (GM-CSF, MIP-1 α , IL-10, IL-1 α , RANTES, VEGF-A, and CXCL9) are altered in the CSF, plasma or brains of AD patients or have AD-associated polymorphisms [66, 74, 79, 86, 120, 121, 125, 136]. GM-CSF, MIP-1 α , MIP-1 β , and CXCL9, IL-10 and VEGF-A are increased in the media of LINE-1 overexpressing iMG. GM-CSF, MIP-1 α , MIP-1 β , and CXCL9 are associated with immune and inflammatory responses [9, 93, 96]. VEGF-A levels were found to be elevated in the CSF and prefrontal cortex of AD patients compared to controls [79, 117], and its protein expression is associated with increased blood brain barrier permeability and tangle pathology [79].

Intriguingly, the most significant difference was the upregulation of the anti-inflammatory cytokine IL-10 in LINE-1⁺ iMG. IL-10 suppresses immune responses through downregulation of proinflammatory signaling and inhibition of major histocompatibility (MHC) class II expression [18, 64], and is elevated in AD patient brains [22, 41]. Studies in AD mouse models have found that IL-10 overexpression exacerbates memory dysfunction, impairs A β phagocytosis and promotes plaque burden [13], and conversely, IL-10 deficiency promotes A β clearance, preserves synaptic integrity, and limits cognitive impairment [41]. Our data demonstrate that increased LINE-1 activity can disrupt typical immune homeostasis and cytokine signaling, and many of these changes parallel those observed in the AD brain.

Elevated LINE-1 activity in iMG impairs phagocytosis of A β ₄₂

Appropriate phagocytic function of microglia is critical in maintaining healthy brain homeostasis. Deficient phagocytic clearance and the accumulation of neurotoxic, aggregate-prone proteins is a feature common to multiple age-related neurodegenerative disease. Microglia display defective phagocytic clearance of amyloid beta (A β) fragments and other substrates in both aging and in LOAD [32, 80, 100],

Fig. 5 Increased LINE-1 activity drives altered immune response in iMG. **A** Volcano plot with data from multiplex array measuring cytokine concentration levels in supernatants from NT control and LINE-1 overexpressing iMG. Labeled cytokines indicate a significant ($p < 0.05$) difference in the concentration of the given cytokine between NT and LINE-1 overexpressing iMG. P values have been adjusted using the Benjamini–Hochberg FDR correction procedure. Dashed line indicates a LFC of 0.5. **B** Representative microscopy images of $A\beta_{42}$ phagocytosis in NT control, NT control + Cytochalasin D, and LINE-1⁺ iMG. **C** Quantification of phagocytosis. $n = 3$ biologically independent experiments. An average of 265 iMG were analyzed per iMG line for each condition. **D** Histograms (flowcytometry) showing proportion of $A\beta_{42}$ -positive and negative cells in both populations. **E** Quantification of percentage differences in flow. Data are presented as mean \pm S.D. and analyzed using an unpaired two-tailed t test; * $P \leq 0.05$; ** $P \leq 0.01$. Exact P values can be found in source text. Scale bar represents 50 μm . LFC log fold change



leading to the development of its characteristic extracellular amyloid plaques [32]. Given our observation of increased LINE-1 expression in LOAD patient microglia, we speculated that LINE-1 overexpression may disrupt microglial phagocytosis of A β . Our findings of dysregulated immune signaling and morphological changes in the LINE-1+ microglia support the hypothesis that LINE-1 activity could compromise microglial phagocytic ability, potentially as part of a broader alteration in microglial phenotype.

To investigate this, we incubated NT-iMG or LINE-1+ iMG with fluorescently labeled A β ₄₂ (A β -647) for 2 h and then analyzed uptake. Through microscopy, we found a roughly threefold reduction in A β ₄₂ internalization, measured through mean fluorescent intensity of conjugated A β ₄₂-647 in LINE-1+ iMG compared to NT control. ($p=0.0021$) (Fig. 5b, c). These results were corroborated through flow cytometry, where we found a significantly reduced percentage of A β ₄₂-positive cells in the LINE-1+ iMG population compared to NT control. ($p=0.0172$) (Fig. 5d, 5e) To confirm the efficacy of our assay, we also pre-incubated a set of iMG with Cytochalasin D, an inhibitor of actin polymerization, before A β ₄₂ incubation and confirmed that A β ₄₂ internalization was largely abolished ($p=0.0016$). Our findings suggest a reduced capacity of LINE-1+ iMG to phagocytose A β ₄₂. While this observation could also reflect increased uptake and subsequent degradation of A β ₄₂ by LINE-1+ microglia within the assessed timeframe, the diminished A β signal, alongside the observed increase in IL-10 expression, most likely indicates that LINE-1 overexpression impairs the microglial ability to phagocytose A β ₄₂. These data thus posit that the LOAD-related decline in phagocytic clearance of amyloid beta could be, in part, due to increased LINE-1 retrotransposon activity in microglia.

LINE-1+ iMG transcriptome reveals changes in lipid metabolism and antigen presentation

To approach a broader, unbiased examination of how LINE-1 overexpression influences microglial state and function, we performed transcriptomics on the LINE-1+ and NT-iMG (Fig. 6a, Supplementary Table 3, and supplementary Fig. 6). Strikingly, we found a strong downregulation of various MHC class II and associated genes in the LINE-1+ iMG, including a pronounced reduction in *HLA-DRA*, *HLA-DRB1*, *HLA-DPB1*, *CD74*, *HLA-DRB5*, *HLA-DQB1*, and *CIITA*. We validated several of the strongest transcriptomic hits through qPCR, (Fig. 6b), confirming the most prominent hits from our transcriptomic analysis.

We used Enrichr (see Supplementary Table 4 for gene list used) to conduct gene ontology (GO) analysis on our differentially expressed genes (DEGs). We found that genes upregulated in LINE-1+ iMG are primarily enriched for genes associated with lipoprotein particle binding and

cholesterol homeostasis, including *APOE*, *LRPI*, *APOC1*, *PLTP*, *THBS1* and *SORL1* (Fig. 6c). These results are intriguing due to the mounting focus on lipid dysregulation in AD [14, 134], and in particular, an association between higher risk of AD development and levels of low-density lipoprotein cholesterol (LDL-c) [101, 138]. We also utilized the Database of Genotypes and Phenotypes (dbGaP) to examine which phenotypes and diseases are enriched with the DEGs upregulated in the LINE-1+ iMG. The analysis identified gene involved in lipid metabolism, cholesterol, HDL and LDL lipoproteins, and AD as the traits that are most enriched with our DEGs (Fig. 6e). Consistent with this, some of the lipoprotein-associated genes enriched in LINE-1+ iMG have been previously linked to AD, such as *APOE* and *LRPI*. In addition to being the strongest genetic risk factor for AD, *APOE* plays critical roles in lipid transport and homeostasis and is a ligand for several low-density lipoprotein receptors [51, 98]. Notably, microglia expressing the *APOE* ϵ 4 risk allele exhibit reduced A β ₄₂ clearance and amoeboid morphology [67], paralleling our observations in LINE-1+ iMG.

Genes in the LINE-1+ downregulated set were enriched for genes involved in the MHC class II protein complex binding and receptor activity (Fig. 6c). MHC II molecules play various roles in inflammation and immune recognition [19, 128]. Reduced MHC II expression may affect microglial ability to act as an antigen presenting cell, minimizing the expansion of CNS immune responses against A β ₄₂. Interestingly, previous studies have identified a microglial subpopulation enriched in antigen presentation genes, including *CD74* and *HLA* genes, which is depleted in the cortex of AD patients [92], paralleling the loss of this signature in the LINE-1+ iMG.

We next examined whether LINE-1 overexpression in iMG impacted expression of AD-associated genes extracted from prior literature. We found that a large number of genes implicated in AD were differentially expressed in LINE-1+ iMG, (Fig. 6d) including the AD risk genes triggering receptor expressed on myeloid cells 2 (*TREM2*) and Abelson interactor family member 3 (*ABI3*), which were reduced in the LINE-1+ iMG. *TREM2* encodes a receptor which mediates several microglial functions, including inflammatory signaling, lipid metabolism, and phagocytosis of A β ₄₂ and other substrates [73]. *ABI3* encodes a protein which plays a role in actin cytoskeleton rearrangement and is required for normal microglial migration and phagocytosis [55, 56, 111].

Altogether, the altered transcriptomic signature of LINE-1+ iMG demonstrates an impact of retrotransposition in various critical microglial functions linked to AD pathogenesis.

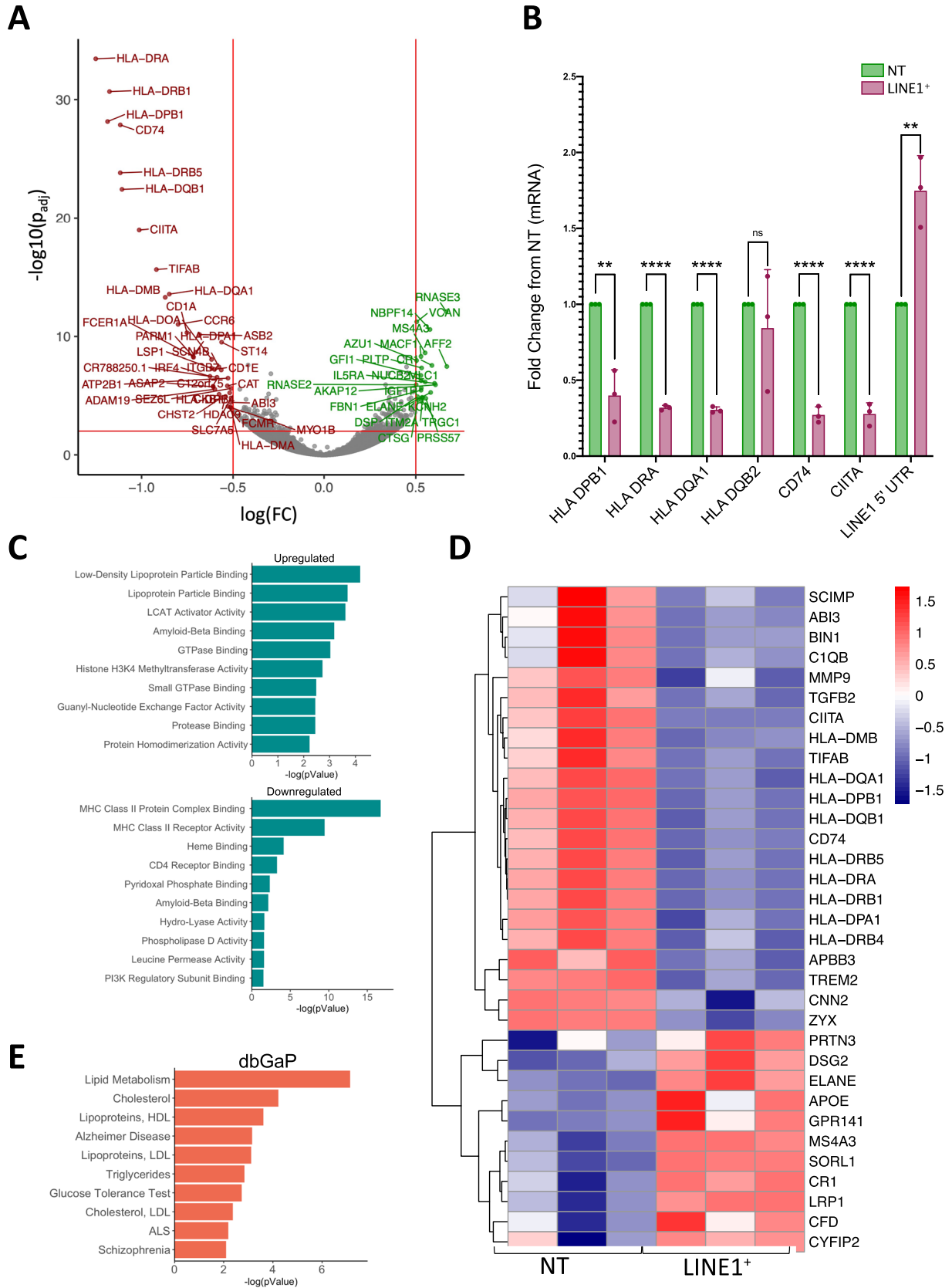


Fig. 6 Transcriptomic analysis of LINE-1⁺ iMG reveal compromised antigen presentation. **A** Volcano plot highlighting differential expression of LINE-1⁺ iMG compared to NT control iMG, analyzed using DESeq2. *n* = 3 biologically independent experiments. **B** qPCR validation of several top differentially expressed hits. *n* = 3 biologically independent experiments. **C** GO analysis of top 100 most significant differentially expressed hits upregulated and downregulated in LINE-1⁺ iMG using Enrichr examining Molecular Function GO terms. **D** Heatmap showing gene expression variation (*Z* score) for selected AD-associated genes between control and LINE-1 overexpressing iMG. **E** Enrichr-based GO analysis of top 100 upregulated hits using dbGaP database to identify phenotypes associated with LINE-1⁺ transcriptional signature. Data are presented as mean ± S.D. and analyzed using an unpaired two-tailed *t* test; **P* ≤ 0.05; ***P* ≤ 0.01, ****P* ≤ 0.001, *****P* ≤ 0.0001, *ns* not significant. Scale bar represents 50 μM. *FC* fold change

Discussion

Age is the primary risk factor for Alzheimer's disease, however the mechanism by which age-related changes contribute to disease pathology remains under investigation. Recently, a role for transposable element activation in aged and senescent cells in driving nervous system dysfunction has emerged. Widespread epigenetic changes have been documented with aging, such as global heterochromatin loss and redistribution [70], which can lead to a permissive environment for transcription of retrotransposable elements such as LINE-1. Importantly, studies examining differences between young and aged microglia repeatedly identify disruptions in chromatin organization and epigenetic regulation in aging, two processes that are highly associated with increased retrotransposon activity [30]. This process of epigenetic aging may be even further dysregulated in AD [88]. Given the disruptive capacity of LINE-1 retrotransposon activity to cell types of the brain, we sought to explore the hypothesis that age-induced LINE-1 mobilization may contribute to disease-associated phenotypes in Alzheimer's disease.

We demonstrate that cell types across the central nervous system in the aged brain possess active LINE-1 copies and that LINE-1 ORF1p expression is higher in microglia from LOAD patients compared to controls. We show that increased LINE-1 expression is associated with activated microglial morphology in patient brain samples. Additionally, our data substantiate prior studies identifying a link between tau pathology and TE dysregulation in neurons [31, 39, 42, 58, 116]. Using an *in vitro* model of increased LINE-1 activity in microglia, we determine that retrotransposon activity disrupts numerous microglial functions and features: morphology, cytokine profile, phagocytic function, lipid metabolism and expression of the antigen presenting machinery. Our data establish a prospective role of LINE-1-mediated microglial dysfunction in LOAD pathology meriting deeper investigation.

Our findings suggest that LINE-1 dysregulation drives microglial dysfunction, such as a blunted phagocytic response to Aβ challenge and downregulation of MHC class II molecules. As previous studies in human fibroblasts found that LINE-1 derepression stimulated inflammation [12], the strong upregulation of IL-10 was unexpected. We speculate that prolonged production of endogenous immunostimulatory extranuclear LINE-1 nucleic acids through persistent retrotransposition may induce immune tolerance programs mediated by IL-10 and promote an immunosuppressive phenotype [61, 129].

It is increasingly clear that a careful balance of microglial function at different stages of aging is critical to ensure cognitive health [65]. Longitudinal studies suggest there may be two peaks of microglial activation over the course of AD progression [28, 38, 43], and there is evidence that early microglial activation in the prodromal stage of AD may be protective [114]. Failure to mount an appropriate immune response during the initial stages of pathology could contribute to the development of aggregates, such as amyloid plaques. In the later stages of AD, these aggregates provoke detrimental microglial activation. This hypothesis is supported by the fact that variants protective against AD, such as the P522R polymorphism of *PLCG2*, is associated with a mild, lifelong increase in microglial activation, antigen presentation, phagocytosis and inflammatory signaling [3, 16, 77, 78, 113, 122], implying that an earlier, potentiated immune response can prevent the initial pathology from developing. We speculate that conversely, prolonged immune dysfunction caused by increased LINE-1 could compromise these early responses and drive AD progression.

Higher rates of somatic mutations have also been reported in Alzheimer's disease [83, 84, 94]. LINE-1 mobilization, by nature, causes endogenous mutagenesis and genome instability. *De novo* LINE-1 insertions initiate and drive progression in several cancers [44], and LINE-1 hypomethylation correlates with cancer risk and worse prognosis [133]. Given the significant genetic component of LOAD (which has a heritability of 58–79%) and the involvement of multiple genetic loci [110], LINE-1-mediated mutagenesis may also contribute to AD development. Intriguingly, LINE-1-driven somatic mosaicism has been documented in both human and mouse neurons and accumulating data suggests this activity contributes to driving neuronal transcriptome complexity and functional diversification important for brain function [8, 17, 25–27, 87, 124]. Our identification of LINE-1 expression in glial cells raises the question of whether LINE-1 activity may be important for establishing transcriptome diversity or heterogeneity in glia.

While this study proposes an exciting role for LINE-1 activity in microglia and neurons in LOAD, we recognize potential limitations to this work. To assess the impact of LINE-1 on microglial function, we induced its

overexpression in iMG and studied relatively acute effects, as iMG in culture last for a limited number of weeks. In LOAD, this activity may occur over the course of decades, and the long-term impact of activity may differ from the acute. Ideally, we would complement our gain-of-function experiments with testing the impact of LINE-1 repression in microglia. However, we detected little to no baseline LINE-1 activity in our iMG system, making it difficult to explore the effects of its repression. Our in vitro system investigated iMG in isolation to specifically study its role in microglia, but future investigations in multi-cell, organoid or in vivo systems may deepen our understanding of its physiological role. As we only had access to postmortem LOAD tissue, we are unable to examine at which point of LOAD progression our observed differences in LINE-1 activity develop. Intriguingly, a recent report found massive dysregulation of TEs, including significant overexpression of LINE-1, immediately preceding the clinical manifestation of amnesic mild cognitive impairment (aMCI) or LOAD [75]. This aligns with our hypothesis that LINE-1 dysregulation is an early event in LOAD and its reactivation occurs with age. Our findings suggest that LINE-1 activity at this stage may impair microglial functions, such as A β clearance, potentially driving increased amyloid plaque burden. Examining a possible correlation between microglial LINE-1 expression and amyloid plaque burden in AD patients would be valuable. Although technical constraints prevented us from probing this relationship in our samples, prior studies have shown associations between transcription of certain TEs and amyloid pathology [42]. Future studies should investigate how LINE-1 dysregulation and amyloid pathology correlate over disease progression.

Overall, our findings identify LINE-1 activity as a novel element underlying microglial and immune dysfunction in LOAD and expand our understanding of how epigenetic dysregulation in aging can contribute to neurodegeneration. These discoveries conceive a potential role for therapeutics promoting protective epigenetic regulation of TEs or inhibiting retrotransposition as successful treatments in Alzheimer's disease.

Supplementary Information The online version contains supplementary material available at <https://doi.org/10.1007/s00401-024-02835-6>.

Acknowledgements We thank the members of the Center for Translational & Computational Neuroimmunology and Taub Institute for Research on Alzheimer's Disease and Aging Brain for technical assistance and helpful discussions. The Neuroimmunology Core is supported by the National Institute on Aging (NIA), part of the National Health Institute (NIH) grant number P30AG066462. ROSMAP is supported by P30AG10161, P30AG72975, R01AG15819, R01AG17917, U01AG46152, U01AG61356. Flow Core Facility is supported by NIH grants: S10OD020056 and S10RR027050. M Olah is supported by R01AG072471.

Authors' contributions N.R., and F.S. conceptualized the study. N.R., I.Haq., and J.C.N. performed the experiments. Nainika Roy, David A. Bennett, Andrew Teich, Philip L. De Jager, Marta Olah, and Falak Sher validated the project. Nainika Roy performed formal analysis and provided visualizations. Nainika Roy and Falak Sher wrote the original draft. All authors reviewed and edited the manuscript. Falak Sher supervised the research, served as the project administrator, and acquired funding.

Funding F. Sher and this study are supported by the National Institute on Aging (NIA), part of the National Health Institute (NIH) grant number R01AG070118, U01 AG06135, and Thompson Family Foundation Program for Accelerated Medicines Exploration in Alzheimer's Disease and Related Disorders of The Nervous System (TAME-AD).

Data Availability The processed RNA-Seq data are provided in the supplementary material, and the original files have been uploaded to the Gene Expression Omnibus (GEO) under accession number GSE276905. ROSMAP data can be requested at www.radc.rush.edu.

Declarations

Conflict of interest The authors declare no competing interests.

Ethics approval and consent to participate The research was conducted in accordance with the guidelines of Institutional Review Board (IRB) of Columbia University New York under protocol AAAR4962. This study utilized induced pluripotent stem cell (iPSC)-derived microglia, hence no direct human participants were involved. Human iPSC lines C1-iPSC (Gibco, catalog A18945), C2-iPSC (ATCC, catalog no. ACS-1024), and CU-iPSC (Columbia Stem Cell Initiative core facility), were obtained in accordance with ethical guidelines for research.

Consent for publication This manuscript does not contain data from individuals necessitating consent for publication.

Open Access This article is licensed under a Creative Commons Attribution-NonCommercial-NoDerivatives 4.0 International License, which permits any non-commercial use, sharing, distribution and reproduction in any medium or format, as long as you give appropriate credit to the original author(s) and the source, provide a link to the Creative Commons licence, and indicate if you modified the licensed material. You do not have permission under this licence to share adapted material derived from this article or parts of it. The images or other third party material in this article are included in the article's Creative Commons licence, unless indicated otherwise in a credit line to the material. If material is not included in the article's Creative Commons licence and your intended use is not permitted by statutory regulation or exceeds the permitted use, you will need to obtain permission directly from the copyright holder. To view a copy of this licence, visit <http://creativecommons.org/licenses/by-nc-nd/4.0/>.

References

1. Akiyama H, Barger S, Barnum S, Bradt B, Bauer J, Cole GM et al (2000) Inflammation and Alzheimer's disease. *Neurobiol Aging* 21:383–421. [https://doi.org/10.1016/S0197-4580\(00\)00124-X](https://doi.org/10.1016/S0197-4580(00)00124-X)
2. del Alajandra C, Alonso IG-I& KI (1996) Alzheimer's disease hyperphosphorylated tau sequesters normal tau into tangles of filaments and disassembles microtubules. *Nat Med* 2:783–787

3. Andreone BJ, Przybyla L, Llapashtica C, Rana A, Davis SS, van Lengerich B et al (2020) Alzheimer's-associated PLCγ2 is a signaling node required for both TREM2 function and the inflammatory response in human microglia. *Nat Neurosci* 23:927–938. <https://doi.org/10.1038/s41593-020-0650-6>
4. Bachiller S, del Pozo-Martín Y, Carrión ÁM (2017) L1 retrotransposition alters the hippocampal genomic landscape enabling memory formation. *Brain Behav Immun* 64:65–70. <https://doi.org/10.1016/j.bbi.2016.12.018>
5. Baillie JK, Barnett MW, Upton KR, Gerhardt DJ, Richmond TA, De Sapio F et al (2011) Somatic retrotransposition alters the genetic landscape of the human brain. *Nature* 479:534. <https://doi.org/10.1038/NATURE10531>
6. Bennett DA, Schneider JA, Arvanitakis Z, Wilson RS (2012) Overview and findings from the religious orders study. *Curr Alzheimer Res* 9:628–645. <https://doi.org/10.2174/156720512801322573>
7. Bennett DA, Schneider JA, Buchman AS, Barnes LL, Boyle PA, Wilson RS (2012) Overview and findings from the rush memory and aging project. *Curr Alzheimer Res* 9:646–663. <https://doi.org/10.2174/156720512801322663>
8. Bodea GO, Botto JM, Ferreiro ME, Sanchez-Luque FJ, de los Rios Barreda J, Rasmussen J, Rahman MA, Fenlon LR, Jansz N, Gubert C, Gerdes P, Bodea L-G, Ajjikuttira P, Da Costa Guevara DJ, Cumner L, Bell CC, Kozulin P, Billon V, Morell S, Kempen M-JHC, Love CJ, Saha K, Palmer LM, Ewing AD, Jhaveri DJ, Richardson SR, Hannan AJ, Faulkner GJ (2024) LINE-1 retrotransposons contribute to mouse PV interneuron development. *Nat Neurosci* 2024:1–11. <https://doi.org/10.1038/s41593-024-01650-2>
9. Boissière-Michot F, Lazennec G, Frugier H, Jarlier M, Roca L, Duffour J et al (2014) Characterization of an adaptive immune response in microsatellite-unstable colorectal cancer. *Oncoimmunology*. <https://doi.org/10.4161/onci.29256>
10. Bray NL, Pimentel H, Melsted P, Pachter L (2016) Near-optimal probabilistic RNA-seq quantification. *Nat Biotechnol* 34:525–527. <https://doi.org/10.1038/nbt.3519>
11. De Cecco M, Criscione SW, Peterson AL, Neretti N, Sedivy JM, Kreiling JA (2013) Transposable elements become active and mobile in the genomes of aging mammalian somatic tissues. *Aging* 5:867–883. <https://doi.org/10.18632/AGING.100621>
12. De Cecco M, Ito T, Petrashen AP, Elias AE, Skvir NJ, Criscione SW et al (2019) L1 drives IFN in senescent cells and promotes age-associated inflammation. *Nature* 566:73–78. <https://doi.org/10.1038/s41586-018-0784-9>
13. Chakrabarty P, Li A, Ceballos-Diaz C, Eddy JA, Funk CC, Moore B et al (2015) IL-10 alters immunoproteostasis in APP mice, increasing plaque burden and worsening cognitive behavior. *Neuron* 85:519–533. <https://doi.org/10.1016/j.neuron.2014.11.020>
14. Chew H, Solomon VA, Fonteh AN (2020) Involvement of lipids in Alzheimer's disease pathology and potential therapies. *Front Physiol* 11:539026. <https://doi.org/10.3389/fphys.2020.00598/BIBTEX>
15. Chomiak AA, Guo Y, Kopsidas CA, McDaniel DP, Lowe CC, Pan H et al (2022) Nde1 is required for heterochromatin compaction and stability in neocortical neurons. *iScience*. <https://doi.org/10.1016/j.isci.2022.104354>
16. Claes C, England WE, Danhash EP, Kiani Shabestari S, Jairaman A, Chadarevian JP et al (2022) The P522R protective variant of PLCG2 promotes the expression of antigen presentation genes by human microglia in an Alzheimer's disease mouse model. *Alzheimers Dement*. <https://doi.org/10.1002/ALZ.12577>
17. Coufal NG, Garcia-Perez JL, Peng GE, Yeo GW, Mu Y, Lovci MT et al (2009) L1 retrotransposition in human neural progenitor cells. *Nature* 460:1127. <https://doi.org/10.1038/NATURE08248>
18. Couper KN, Blount DG, Riley EM (2008) IL-10: the master regulator of immunity to infection. *J Immunol* 180:5771–5777. <https://doi.org/10.4049/JIMMUNOL.180.9.5771>
19. Das R, Chinnathambi S (2019) Microglial priming of antigen presentation and adaptive stimulation in Alzheimer's disease. *Cell Mol Life Sci* 76:3681–3694. <https://doi.org/10.1007/S00018-019-03132-2>
20. Davies DS, Ma J, Jegathees T, Goldsbury C (2017) Microglia show altered morphology and reduced arborization in human brain during aging and Alzheimer's disease. *Brain Pathol* 27:795. <https://doi.org/10.1111/BPA.12456>
21. De Jager PL, Srivastava G, Lunnon K, Burgess J, Schalkwyk LC, Yu L et al (2014) Alzheimer's disease: early alterations in brain DNA methylation at ANK1, BIN1, RHBDF2 and other loci. *Nat Neurosci* 17:1156–1163. <https://doi.org/10.1038/nn.3786>
22. Doecke JD, Laws SM, Faux NG, Wilson W, Burnham SC, Lam CP et al (2012) Blood-based protein biomarkers for diagnosis of Alzheimer disease. *Arch Neurol* 69:1318. <https://doi.org/10.1001/ARCHNEUROL.2012.1282>
23. Doucet-O'Hare TT, Rodić N, Sharma R, Darbari I, Abril G, Choi JA et al (2015) LINE-1 expression and retrotransposition in Barrett's esophagus and esophageal carcinoma. *Proc Natl Acad Sci USA* 112:E4894–E4900. <https://doi.org/10.1073/pnas.1502474112>
24. Doyle GA, Crist RC, Karatas ET, Hammond MJ, Ewing AD, Ferraro TN et al (2017) Analysis of LINE-1 elements in dna from postmortem brains of individuals with schizophrenia. *Neuropsychopharmacology* 42:2602. <https://doi.org/10.1038/NPP.2017.115>
25. Erwin JA, Paquola ACM, Singer T, Gallina I, Novotny M, Quayle C et al (2016) L1-associated genomic regions are deleted in somatic cells of the healthy human brain. *Nat Neurosci* 19:1583. <https://doi.org/10.1038/NN.4388>
26. Evrony GD, Cai X, Lee E, Hills LB, Elhosary PC, Lehmann HS et al (2012) Single-neuron sequencing analysis of L1 retrotransposition and somatic mutation in the human brain. *Cell* 151:483–496. <https://doi.org/10.1016/j.cell.2012.09.035>
27. Evrony GD, Lee E, Mehta BK, Benjamini Y, Johnson RM, Cai X et al (2015) Cell lineage analysis in human brain using endogenous retroelements. *Neuron* 85:49–59. <https://doi.org/10.1016/j.neuron.2014.12.028>
28. Fan Z, Brooks DJ, Okello A, Edison P (2017) An early and late peak in microglial activation in Alzheimer's disease trajectory. *Brain* 140:792. <https://doi.org/10.1093/BRAIN/AWW349>
29. Felsky D, Roostaei T, Nho K, Risacher SL, Bradshaw EM, Petyuk V et al (2019) Neuropathological correlates and genetic architecture of microglial activation in elderly human brain. *Nat Commun*. <https://doi.org/10.1038/s41467-018-08279-3>
30. Flowers A, Bell-Temin H, Jalloh A, Stevens SM, Bickford PC (2017) Proteomic analysis of aged microglia: shifts in transcription, bioenergetics, and nutrient response. *J Neuroinflamm* 14:96. <https://doi.org/10.1186/s12974-017-0840-7>
31. Frost B, Hemberg M, Lewis J, Feany MB (2014) Tau promotes neurodegeneration through global chromatin relaxation. *Nat Neurosci* 17:357. <https://doi.org/10.1038/NN.3639>
32. Gabandé-Rodríguez E, Keane L, Capasso M (2020) Microglial phagocytosis in aging and Alzheimer's disease. *J Neurosci Res* 98:284–298. <https://doi.org/10.1002/JNR.24419>
33. Garza R, Atacho DAM, Adami A, Gerdes P, Vinod M, Hsieh PH et al (2023) LINE-1 retrotransposons drive human neuronal transcriptome complexity and functional diversification. *Sci Adv*. <https://doi.org/10.1126/SCIADV.ADH9543>
34. Ge SX, Son EW, Yao R (2018) iDEP: an integrated web application for differential expression and pathway analysis of

- RNA-Seq data. *BMC Bioinform* 19:534. <https://doi.org/10.1186/s12859-018-2486-6>
35. Goodier JL, Zhang L, Vetter MR, Kazazian HH (2007) LINE-1 ORF1 protein localizes in stress granules with other RNA-binding proteins, including components of RNA interference RNA-induced silencing complex. *Mol Cell Biol* 27:6469–6483. https://doi.org/10.1128/MCB.00332-07/SUPPL_FILE/MCBSUPPLDATA.ZIP
 36. Gorbunova V, Seluanov A, Mita P, McKerrow W, Fenyö D, Boeke JD et al (2021) The role of retrotransposable elements in ageing and age-associated diseases. *Nature* 596:43–53. <https://doi.org/10.1038/s41586-021-03542-y>
 37. Grabert K, Michael T, Karavolos MH, Clohisey S, Kenneth Bailly J, Stevens MP et al (2016) Microglial brain region-dependent diversity and selective regional sensitivities to aging. *Nat Neurosci* 19:504–516. <https://doi.org/10.1038/nn.4222>
 38. Green GS, Fujita M, Yang H-S, Taga M, McCabe C, Cain A et al (2023) Cellular dynamics across aged human brains uncover a multicellular cascade leading to Alzheimer's disease. *bioRxiv*. <https://doi.org/10.1101/2023.03.07.531493>
 39. Grundman J, Spencer B, Sarsoza F, Rissman RA (2021) Transcriptome analyses reveal tau isoform-driven changes in transposable element and gene expression. *PLoS One* 16:e0251611. <https://doi.org/10.1371/JOURNAL.PONE.0251611>
 40. Guerreiro R, Bras J (2015) The age factor in Alzheimer's disease. *Genome Med* 7:1–3. <https://doi.org/10.1186/S13073-015-0232-5>
 41. Guillot-Sestier MV, Doty KR, Gate D, Rodriguez J, Leung BP, Rezai-Zadeh K et al (2015) I110 deficiency rebalances innate immunity to mitigate Alzheimer-like pathology. *Neuron* 85:534–548. <https://doi.org/10.1016/j.neuron.2014.12.068>
 42. Guo C, Jeong HH, Hsieh YC, Klein HU, Bennett DA, De Jager PL et al (2018) Tau activates transposable elements in Alzheimer's disease. *Cell Rep* 23:2874–2880. <https://doi.org/10.1016/j.celrep.2018.05.004/ATTACHMENT/170D5AD6-B9DA-4FCB-9F66-DA0A01790050/MMC3.XLSX>
 43. Hamelin L, Lagarde J, Dorothée G, Potier MC, Corlier F, Kuhnast B et al (2018) Distinct dynamic profiles of microglial activation are associated with progression of Alzheimer's disease. *Brain* 141:1855–1870. <https://doi.org/10.1093/BRAIN/AWY079>
 44. Hancks DC, Kazazian HH (2016) Roles for retrotransposon insertions in human disease. *Mob DNA* 7:1–28. <https://doi.org/10.1186/S13100-016-0065-9>
 45. Hanseuw BJ, Betensky RA, Jacobs HIL, Schultz AP, Sepulcre J, Becker JA et al (2019) Association of amyloid and tau with cognition in preclinical Alzheimer disease: a longitudinal study. *JAMA Neurol* 76:915–924. <https://doi.org/10.1001/jamaneurol.2019.1424>
 46. Haq I, Ngo JC, Roy N, Pan RL, Nawsheen N, Chiu R et al (2024) An integrated toolkit for human microglia functional genomics. *Stem Cell Res Ther* 15:104. <https://doi.org/10.1186/s13287-024-03700-9>
 47. Heppner FL, Ransohoff RM, Becher B (2015) Immune attack: the role of inflammation in Alzheimer disease. *16*. <https://doi.org/10.1038/nrn3880>
 48. Heyn H, Li N, Ferreira HJ, Moran S, Pisano DG, Gomez A et al (2012) Distinct DNA methylomes of newborns and centenarians. *Proc Natl Acad Sci USA* 109:10522–10527. https://doi.org/10.1073/PNAS.1120658109/SUPPL_FILE/SD05.XLSX
 49. Hopperton KE, Mohammad D, Trépanier MO, Giuliano V, Bazinet RP (2017) Markers of microglia in post-mortem brain samples from patients with Alzheimer's disease: a systematic review. *Mol Psychiatr* 23:177–198. <https://doi.org/10.1038/mp.2017.246>
 50. Huang CRL, Schneider AM, Lu Y, Niranjana T, Shen P, Robinson MA et al (2010) Mobile interspersed repeats are major structural variants in the human genome. *Cell* 141:1171–1182. <https://doi.org/10.1016/J.CELL.2010.05.026>
 51. Husain MA, Laurent B, Plourde M (2021) APOE and Alzheimer's disease: from lipid transport to physiopathology and therapeutics. *Front Neurosci* 15:1. <https://doi.org/10.3389/FNINS.2021.630502>
 52. Iskow RC, McCabe MT, Mills RE, Torene S, Pittard WS, Newwald AF et al (2010) Natural mutagenesis of human genomes by endogenous retrotransposons. *Cell* 141:1253–1261. <https://doi.org/10.1016/J.CELL.2010.05.020>
 53. Jintaridith P, Mutirangura A (2010) Distinctive patterns of age-dependent hypomethylation in interspersed repetitive sequences. *Physiol Genom* 41:194–200. https://doi.org/10.1152/PHYSIOLGENOMICS.00146.2009/SUPPL_FILE/SUPPDATA.PDF
 54. Jönsson ME, Ludvik Brattås P, Gustafsson C, Petri R, Yudovich D, Pircs K et al (2019) Activation of neuronal genes via LINE-1 elements upon global DNA demethylation in human neural progenitors. *Nat Commun* 10:1–11. <https://doi.org/10.1038/s41467-019-11150-8>
 55. Karahan H, Smith DC, Kim B, Dabin LC, Al-Amin MM, Sagara Wijeratne HR et al (2021) Deletion of Abi3 gene locus exacerbates neuropathological features of Alzheimer's disease in a mouse model of A β amyloidosis. *Sci Adv* 7:3954. <https://doi.org/10.1126/SCIADV.ABE3954>
 56. Karahan H, Smith DC, Kim B, McCord B, Mantor J, John SK et al (2023) The effect of Abi3 locus deletion on the progression of Alzheimer's disease-related pathologies. *Front Immunol* 14:1102530. <https://doi.org/10.3389/FIMMU.2023.1102530/BIBTEX>
 57. Keren-Shaul H, Spinrad A, Weiner A, Matcovitch-Natan O, Dvir-Szternfeld R, Ulland TK et al (2017) A unique microglia type associated with restricting development of Alzheimer's disease. *Cell* 169:1276–1290.e17. <https://doi.org/10.1016/j.cell.2017.05.018>
 58. Klein HU, McCabe C, Gjonneska E, Sullivan SE, Kaskow BJ, Tang A et al (2018) Epigenome-wide study uncovers large-scale changes in histone acetylation driven by tau pathology in aging and Alzheimer's human brains. *Nat Neurosci* 22:37–46. <https://doi.org/10.1038/s41593-018-0291-1>
 59. Konermann S, Brigham MD, Trevino AE, Joung J, Abudayyeh OO, Barcena C et al (2015) Genome-scale transcriptional activation by an engineered CRISPR-Cas9 complex. *Nature* 517:583–588. <https://doi.org/10.1038/nature14136>
 60. Krabbe G, Halle A, Matyash V, Rinnenthal JL, Eom GD, Bernhardt U et al (2013) Functional impairment of microglia coincides with beta-amyloid deposition in mice with Alzheimer-like pathology. *PLoS One* 8:1. <https://doi.org/10.1371/journal.pone.0060921>
 61. Lajqi T, Lang GP, Haas F, Williams DL, Hudalla H, Bauer M et al (2019) Memory-like inflammatory responses of microglia to rising doses of LPS: key role of PI3K γ . *Front Immunol* 10:475729. <https://doi.org/10.3389/FIMMU.2019.02492/BIBTEX>
 62. Lanciano S, Cristofari G (2020) Measuring and interpreting transposable element expression. *Nat Rev Gen* 21:721–736. <https://doi.org/10.1038/s41576-020-0251-y>
 63. Lander ES, Linton LM, Birren B, Nusbaum C, Zody MC, Baldwin J et al (2001) Initial sequencing and analysis of the human genome. *Nature* 409:860–921. <https://doi.org/10.1038/35057062>
 64. Lau SF, Fu AKY, Ip NY (2021) Cytokine signaling convergence regulates the microglial state transition in Alzheimer's disease. *Cell Mol Life Sci* 78:4703–4712. <https://doi.org/10.1007/S00018-021-03810-0/FIGURES/2>
 65. Leng F, Edison P (2020) Neuroinflammation and microglial activation in Alzheimer disease: where do we go from here? *Nat Rev Neurol* 17:157–172. <https://doi.org/10.1038/s41582-020-00435-y>

66. Li K, Dai D, Yao L, Gu X, Luan K, Tian W et al (2008) Association between the macrophage inflammatory protein-1 alpha gene polymorphism and Alzheimer's disease in the Chinese population. *Neurosci Lett* 433:125–128. <https://doi.org/10.1016/J.NEU-LET.2008.01.002>
67. Lin YT, Seo J, Gao F, Feldman HM, Wen HL, Penney J et al (2018) APOE4 causes widespread molecular and cellular alterations associated with Alzheimer's disease phenotypes in human iPSC-derived brain cell types. *Neuron* 98:1141–1154.e7. <https://doi.org/10.1016/j.neuron.2018.05.008>
68. Liu XL, Hu JY, Hu MY, Zhang Y, Hong ZY, Cheng XQ et al (2015) Sequence-dependent abnormal aggregation of human Tau fragment in an inducible cell model. *Biochim Biophys Acta Mol Basis Dis* 1852:1561–1573. <https://doi.org/10.1016/j.bbadis.2015.04.015>
69. Liu T, Zhang L, Joo D, Sun SC (2017) NF- κ B signaling in inflammation. *Signal Transduct Target Ther*. <https://doi.org/10.1038/sigtrans.2017.23>
70. López-Otín C, Blasco MA, Partridge L, Serrano M, Kroemer G (2013) The hallmarks of aging. *Cell* 153:1194. <https://doi.org/10.1016/J.CELL.2013.05.039>
71. Love MI, Huber W, Anders S (2014) Moderated estimation of fold change and dispersion for RNA-seq data with DESeq2. *Genome Biol* 15:550. <https://doi.org/10.1186/s13059-014-0550-8>
72. Lue LF, Rydel R, Brigham EF, Yang LB, Hampel H, Murphy GM et al (2001) Inflammatory repertoire of Alzheimer's disease and nondemented elderly microglia in vitro. *Glia* 35:72–79. <https://doi.org/10.1002/GLIA.1072>
73. Lue L-F, Schmitz CT, Walker DG (2015) What happens to microglial TREM2 in Alzheimer's disease: immunoregulatory turned into immunopathogenic? *Neuroscience* 302:138–150
74. Ma SL, Tang NLS, Lam LCW, Chiu HFK (2005) The association between promoter polymorphism of the interleukin-10 gene and Alzheimer's disease. *Neurobiol Aging* 26:1005–1010. <https://doi.org/10.1016/J.NEUROBIOLAGING.2004.08.010>
75. Macciardi F, Giulia Bacalini M, Miramontes R, Boattini A, Taccioli C, Modenini G, Malhas R, Anderlucci L, Gusev Y, Thomas ·, Gross J, Padilla RM, Massimo ·, Fiandaca S, Head E, Guffanti G, Federoff HJ, Mapstone M, Macciardi F, Giulia Bacalini M, Miramontes R, Malhas · R, Gross · T J, Padilla · R M, Fiandaca · M S, Federoff · H J, Mapstone · M, Boattini A, Modenini · G, Head E, Guffanti G (2022) A retrotransposon storm marks clinical phenocopy conversion to late-onset Alzheimer's disease. *GeroScience* 44:1525–1550. <https://doi.org/10.1007/S11357-022-00580-W>
76. MacIa A, Widmann TJ, Heras SR, Ayllon V, Sanchez L, Benkaddour-Boumzaouad M et al (2017) Engineered LINE-1 retrotransposition in nondividing human neurons. *Genome Res* 27:335–348. <https://doi.org/10.1101/GR.206805.116/-/DC1>
77. Magno L, Lessard CB, Martins M, Lang V, Cruz P, Asi Y et al (2019) Alzheimer's disease phospholipase C-gamma-2 (PLCG2) protective variant is a functional hypermorph. *Alzheimers Res Ther*. <https://doi.org/10.1186/S13195-019-0469-0>
78. Maguire E, Menzies GE, Phillips T, Sasner M, Williams HM, Czubala MA et al (2021) PIP2 depletion and altered endocytosis caused by expression of Alzheimer's disease-protective variant PLC γ 2 R522. *EMBO J* 40:e105603. <https://doi.org/10.15252/EMBJ.2020105603>
79. Mahoney ER, Dumitrescu L, Moore AM, Cambronerero FE, De Jager PL, Koran MEI et al (2019) Brain expression of the vascular endothelial growth factor gene family in cognitive aging and Alzheimer's disease. *Mol Psychiatry* 26:888–896. <https://doi.org/10.1038/s41380-019-0458-5>
80. Mawuenyega KG, Sigurdson W, Ovod V, Munsell L, Kasten T, Morris JC et al (2010) Decreased clearance of CNS amyloid- β in Alzheimer's disease. *Science* 330:1774. <https://doi.org/10.1126/SCIENCE.1197623>
81. McQuade A, Blurton-Jones M (2019) Microglia in Alzheimer's disease: exploring how genetics and phenotype influence risk. *J Mol Biol* 431:1805. <https://doi.org/10.1016/J.JMB.2019.01.045>
82. Mertens J, Paquola ACM, Ku M, Hatch E, Böhnke L, Ladjevardi S et al (2015) Directly reprogrammed human neurons retain aging-associated transcriptomic signatures and reveal age-related nucleocytoplasmic defects. *Cell Stem Cell* 17:705–718. <https://doi.org/10.1016/j.stem.2015.09.001>
83. Miller MB, Reed HC, Walsh CA (2021) Brain somatic mutation in aging and Alzheimer's disease. *Annu Rev Genomics Hum Genet* 22:239. <https://doi.org/10.1146/ANNUR-REV-GENOM-121520-081242>
84. Miller MB, Huang AY, Kim J, Zhou Z, Kirkham SL, Maury EA et al (2022) Somatic genomic changes in single Alzheimer's disease neurons. *Nature* 604:714–722. <https://doi.org/10.1038/s41586-022-04640-1>
85. Mita P, Wudzinska A, Sun X, Andrade J, Nayak S, Kahler DJ et al (2018) LINE-1 protein localization and functional dynamics during the cell cycle. *Elife*. <https://doi.org/10.7554/ELIFE.30058>
86. Mrak RE, Griffin WST (2000) Interleukin-1 and the immunogenetics of Alzheimer disease. *J Neuropathol Exp Neurol* 59:471. <https://doi.org/10.1093/JNEN/59.6.471>
87. Muotri AR, Chu VT, Marchetto MCN, Deng W, Moran JV, Gage FH (2005) Somatic mosaicism in neuronal precursor cells mediated by L1 retrotransposition. *Nature* 435:903–910. <https://doi.org/10.1038/nature03663>
88. Nativio R, Donahue G, Berson A, Lan Y, Amlie-Wolf A, Tuzer F et al (2018) Dysregulation of the epigenetic landscape of normal aging in Alzheimer's disease. *Nat Neurosci* 21:497–505. <https://doi.org/10.1038/s41593-018-0101-9>
89. Newman SL, Bucher C, Rhodes J, Bullock WE (1990) Phagocytosis of *Histoplasma capsulatum* yeasts and microconidia by human cultured macrophages and alveolar macrophages. Cellular cytoskeleton requirement for attachment and ingestion. *J Clin Invest* 85:223–230. <https://doi.org/10.1172/JCI114416>
90. Nimmerjahn A, Kirchhoff F, Helmchen F (2005) Resting microglial cells are highly dynamic surveillants of brain parenchyma in vivo. *Science* 308:1314–1318. <https://doi.org/10.1126/SCIENCE.1110647>
91. Olah M, Patrick E, Villani AC, Xu J, White CC, Ryan KJ et al (2018) A transcriptomic atlas of aged human microglia. *Nat Commun* 9:1–8. <https://doi.org/10.1038/s41467-018-02926-5>
92. Olah M, Menon V, Habib N, Taga MF, Ma Y, Yung CJ et al (2020) Single cell RNA sequencing of human microglia uncovers a subset associated with Alzheimer's disease. *Nat Commun* 11:1–18. <https://doi.org/10.1038/s41467-020-19737-2>
93. Ousman SS, David S (2001) MIP-1, MCP-1, GM-CSF, and TNF-control the immune cell response that mediates rapid phagocytosis of myelin from the adult mouse spinal cord. *J Neurosci*. <https://doi.org/10.1523/JNEUROSCI.21-13-04649.2001>
94. Park JS, Lee J, Jung ES, Kim MH, Bin Kim I, Son H et al (2019) Brain somatic mutations observed in Alzheimer's disease associated with aging and dysregulation of tau phosphorylation. *Nat Commun* 10:1–12. <https://doi.org/10.1038/s41467-019-11000-7>
95. Patterson KR, Remmers C, Fu Y, Brooker S, Kanaan NM, Vana L et al (2011) Characterization of prefibrillar tau oligomers in vitro and in Alzheimer disease. *J Biol Chem* 286:23063–23076. <https://doi.org/10.1074/jbc.M111.237974>
96. Perales M, Fantuzzi G, Goldberg SM, Turk MJ, Mortazavi F, Busam K et al (2002) GM-CSF DNA induces specific patterns of cytokines and chemokines in the skin: implications for DNA vaccines. *Cytokine Cell Mol Ther* 7:125–133. <https://doi.org/10.1080/13684730310000923>

97. Petersen MA, Dailey ME (2004) Diverse microglial motility behaviors during clearance of dead cells in hippocampal slices. *Glia* 46:195–206. <https://doi.org/10.1002/GLIA.10362>
98. Raulin AC, Doss SV, Trottier ZA, Ikezu TC, Bu G, Liu CC (2022) ApoE in Alzheimer's disease: pathophysiology and therapeutic strategies. *Mol Neurodegen* 17:1–26. <https://doi.org/10.1186/S13024-022-00574-4>
99. Rodić N, Sharma R, Sharma R, Zampella J, Dai L, Taylor MS et al (2014) Long interspersed element-1 protein expression is a hallmark of many human cancers. *Am J Pathol* 184:1280–1286. <https://doi.org/10.1016/j.ajpath.2014.01.007>
100. Safaiyan S, Kannaiyan N, Snaidero N, Brioschi S, Biber K, Yona S et al (2016) Age-related myelin degradation burdens the clearance function of microglia during aging. *Nat Neurosci* 19:995–998. <https://doi.org/10.1038/nn.4325>
101. Sáiz-Vázquez O, Puente-Martínez A, Ubillos-Landa S, Pacheco-Bonrostro J, Santabárbara J (2020) Cholesterol and Alzheimer's disease risk: a meta-meta-analysis. *Brain Sci* 10:1–13. <https://doi.org/10.3390/BRAINS10060386>
102. Sanson KR, Hanna RE, Hegde M, Donovan KF, Strand C, Sullender ME et al (2018) Optimized libraries for CRISPR-Cas9 genetic screens with multiple modalities. *Nat Commun* 9:1–15. <https://doi.org/10.1038/s41467-018-07901-8>
103. Sanson KR, Hanna RE, Hegde M, Donovan KF, Strand C, Sullender ME et al (2018) Optimized libraries for CRISPR-Cas9 genetic screens with multiple modalities. *Nat Commun*. <https://doi.org/10.1038/s41467-018-07901-8>
104. Shahidehpour RK, Higdon RE, Crawford NG, Neltner JH, Ighodaro ET, Patel E et al (2021) Dystrophic microglia are associated with neurodegenerative disease and not healthy aging in the human brain. *Neurobiol Aging* 99:19. <https://doi.org/10.1016/J.NEUROBIOLAGING.2020.12.003>
105. Sharma R, Rodić N, Burns KH, Taylor MS (2016) Immunodetection of human LINE-1 expression in cultured cells and human tissues. *Methods Mol Biol* 1400:261–280. https://doi.org/10.1007/978-1-4939-3372-3_17/FIGURES/4
106. Shireby G, Dempster EL, Policicchio S, Smith RG, Pishva E, Chioza B et al (2022) DNA methylation signatures of Alzheimer's disease neuropathology in the cortex are primarily driven by variation in non-neuronal cell-types. *Nat Commun* 13:1–14. <https://doi.org/10.1038/s41467-022-33394-7>
107. Sil S, Keegan S, Etefa F, Denes LT, Boeke JD, Holt LJ (2022) Condensation of LINE-1 is critical for retrotransposition. *Elife*. <https://doi.org/10.7554/ELIFE.82991>
108. Silva MVF, Loures CDMG, Alves LCV, De Souza LC, Borges KBG, Carvalho MDG (2019) Alzheimer's disease: risk factors and potentially protective measures. *J Biomed Sci* 26:1–11. <https://doi.org/10.1186/S12929-019-0524-Y>
109. Simon M, Van Meter M, Ablava J, Ke Z, Gonzalez RS, Taguchi T et al (2019) LINE1 derepression in aged wild-type and SIRT6-deficient mice drives inflammation. *Cell Metab* 29:871–885.e5. <https://doi.org/10.1016/j.cmet.2019.02.014>
110. Sims R, Hill M, Williams J (2020) The multiplex model of the genetics of Alzheimer's disease. *Nat Neurosci* 23:311–322
111. Sims R, Van Der Lee SJ, Naj AC, Bellenguez C, Badarinarayan N, Jakobsdottir J, Kunkle BW, Boland A, Raybould R, Bis JC, Martin ER, Grenier-Boley B, Heilmann-Heimbach S, Chouraki V, Kuzma AB, Sleegers K, Vronskaya M, Ruiz A, Graham RR, Olaso R, Hoffmann P, Grove ML, Vardarajan BN, Hiltunen M, Nöthen MM, White CC, Hamilton-Nelson KL, Epelbaum J, Maier W, Choi SH, Beecham GW, Dulary C, Herms S, Smith A V., Funk CC, Derbois C, Forstner AJ, Ahmad S, Li H, Bacq D, Harold D, Satizabal CL, Valladares O, Squassina A, Thomas R, Brody JA, Qu L, Sánchez-Juan P, Morgan T, Wolters FJ, Zhao Y, Garcia FS, Denning N, Fornage M, Malamon J, Naranjo MCD, Majounie E, Mosley TH, Dombroski B, Wallon D, Lupton MK, Dupuis J, Whitehead P, Fratiglioni L, Medway C, Jian X, Mukherjee S, Keller L, Brown K, Lin H, Cantwell LB, Panza F, McGuinness B, Moreno-Grau S, Burgess JD, Solfrizzi V, Proitsi P, Adams HH, Allen M, Seripa D, Pastor P, Cupples LA, Price ND, Hannequin D, Frank-García A, Levy D, Chakrabarty P, Caffarra P, Giegling I, Beiser AS, Giedraitis V, Hampel H, Garcia ME, Wang X, Lannfelt L, Mecocci P, Eiriksdottir G, Crane PK, Pasquier F, Boccardi V, Hernández I, Barber RC, Scherer M, Tarraga L, Adams PM, Leber M, Chen Y, Albert MS, Riedel-Heller S, Emilsson V, Beekly D, Braae A, Schmidt R, Blacker D, Masullo C, Schmidt H, Doody RS, Spalletta G, Jr WTL, Fairchild TJ, Bossù P, Lopez OL, Frosch MP, Sacchinelli E, Ghetti B, Yang Q, Huebinger RM, Jessen F, Li S, Kamboh MI, Morris JC, Sotolongo-Grau O, Katz MJ, Corcoran C, Dunstan M, Braddel A, Thomas C, Meggy A, Marshall R, Gerrish A, Chapman J, Aguilar M, Taylor S, Hill M, Fairén MD, Hodges A, Vellas B, Soininen H, Kloszewska I, Daniilidou M, Uphill J, Patel Y, Hughes JT, Lord J, Turton J, Hartmann AM, Cecchetti R, Fenoglio C, Serpente M, Arcaro M, Caltagirone C, Orfei MD, Ciarabella A, Pichler S, Mayhaus M, Gu W, Lleó A, Fortea J, Blesa R, Barber IS, Brookes K, Cupidi C, Maletta RG, Carrell D, Sorbi S, Moebus S, Urbano M, Pilotto A, Kornhuber J, Bosco P, Todd S, Craig D, Johnston J, Gill M, Lawlor B, Lynch A, Fox NC, Hardy J, Albin RL, Apostolova LG, Arnold SE, Asthana S, Atwood CS, Baldwin CT, Barnes LL, Barral S, Beach TG, Becker JT, Bigio EH, Bird TD, Boeve BF, Bowen JD, Boxer A, Burke JR, Burns JM, Buxbaum JD, Cairns NJ, Cao C, Carlson CS, Carlsson CM, Carney RM, Carrasquillo MM, Carroll SL, Diaz CC, Chui HC, Clark DG, Cribbs DH, Crocco EA, Decarli C, Dick M, Duara R, Evans DA, Faber KM, Fallon KB, Fardo DW, Farlow MR, Ferris S, Foroud TM, Galasko DR, Gearing M, Geschwind DH, Gilbert JR, Graff-Radford NR, Green RC, Growdon JH, Hamilton RL, Harrell LE, Honig LS, Huentelman MJ, Hulette CM, Hyman BT, Jarvik GP, Abner E, Jin LW, Jun G, Karydas A, Kaye JA, Kim R, Kowall NW, Kramer JH, Laferla FM, Lah JJ, Leverenz JB, Levey AI, Li G, Lieberman AP, Lunetta KL, Lyketsos CG, Marson DC, Martiniuk F, Mash DC, Masliah E, McCormick WC, McCurry SM, McDavid AN, McKee AC, Mesulam M, Miller BL, Miller CA, Miller JW, Murrell JR, Myers AJ, O'Bryant S, Olichney JM, Pankratz VS, Parisi JE, Paulson HL, Perry W, Peskind E, Pierce A, Poon WW, Potter H, Quinn JF, Raj A, Raskind M, Reisberg B, Reitz C, Ringman JM, Roberson ED, Rogaeva E, Rosen HJ, Rosenberg RN, Sager MA, Saykin AJ, Schneider JA, Schneider LS, Seeley WW, Smith AG, Sonnen JA, Spina S, Stern RA, Swardlow RH, Tanzi RE, Thornton-Wells TA, Trojanowski JQ, Troncoso JC, Van Deerlin VM, Van Eldik LJ, Vinters H V., Vonsattel JP, Weintraub S, Welsh-Bohmer KA, Wilhelmsen KC, Williamson J, Wingo TS, Woltjer RL, Wright CB, Yu CE, Yu L, Garzia F, Golamally F, Septier G, Engelborghs S, Vandenberghe R, De Deyn PP, Fernandez CM, Benito YA, Thonberg H, Forsell C, Lilius L, Kinhult-Ståhlbom A, Kilander L, Brundin R, Concari L, Helisalmi S, Koivisto AM, Haapasalo A, Dermecourt V, Fievet N, Hanon O, Dufouil C, Brice A, Ritchie K, Dubois B, Himali JJ, Keene CD, Tschanz J, Fitzpatrick AL, Kukull WA, Norton M, Aspelund T, Larson EB, Munger R, Rotter JJ, Lipton RB, Bullido MJ, Hofman A, Montine TJ, Coto E, Boerwinkle E, Petersen RC, Alvarez V, Rivadeneira F, Reiman EM, Gallo M, O'Donnell CJ, Reisch JS, Bruni AC, Royall DR, Dichgans M, Sano M, Galimberti D, St George-Hyslop P, Scarpini E, Tsuang DW, Mancuso M, Bonuccelli U, Winslow AR, Daniele A, Wu CK, Peters O, Nacmias B, Riemenschneider M, Heun R, Brayne C, Rubinsztein DC, Bras J, Guerreiro R, Al-Chalabi A, Shaw CE, Collinge J, Tsolaki M, Clarimón J, Sussams R, Lovestone S, O'Donovan MC, Owen MJ, Behrens TW, Mead S, Uitterlinden AG, Holmes C, Cruchaga C, Ingelsson M, Bennett DA, Powell J, Golde TE,

- Graff C, De Jager PL, Morgan K, Ertekin-Taner N, Combarros O, Psaty BM, Passmore P, Younkin SG, Berr C, Gudnason V, Rujescu D, Dickson DW, Dartigues JF, Destefano AL, Ortega-Cubero S, Hakonarson H, Campion D, Boada M, Kauwe JK, Farrer LA, Van Broeckhoven C, Ikram MA, Jones L, Haines JL, Tzourio C, Tzourio C, Escott-Price V, Mayeux R, Deleuze JF, Amin N, Goate AM, Pericak-Vance MA, Amouyel P, Van Duijn CM, Ramirez A, Wang LS, Lambert JC, Seshadri S, Williams J, Schellenberg GD (2017) Rare coding variants in *PLCG2*, *ABI3*, and *TREM2* implicate microglial-mediated innate immunity in Alzheimer's disease. *Nature Genetics* 49:1373–1384. <https://doi.org/10.1038/ng.3916>
112. Sobue A, Komine O, Hara Y, Endo F, Mizoguchi H, Watanabe S et al (2021) Microglial gene signature reveals loss of homeostatic microglia associated with neurodegeneration of Alzheimer's disease. *Acta Neuropathol Commun* 9:1–17. <https://doi.org/10.1186/S40478-020-01099-X/FIGURES/6>
113. Solomon S, Kumar Sampathkumar N, Carre I, Mondal M, Chennell G, Vernon AC, Ruepp M-D, Mitchell J (2022) Heterozygous expression of the Alzheimer's disease protective *PLCγ2* P522R variant enhances Aβ clearance while preserving synapses. <https://doi.org/10.21203/rs.3.rs-1420006/v2>
114. Streit WJ, Braak H, Xue QS, Bechmann I (2009) Dystrophic (senescent) rather than activated microglial cells are associated with tau pathology and likely precede neurodegeneration in Alzheimer's disease. *Acta Neuropathol* 118:475–485. <https://doi.org/10.1007/S00401-009-0556-6/FIGURES/7>
115. Streit WJ, Braak H, Xue QS, Bechmann I (2009) Dystrophic (senescent) rather than activated microglial cells are associated with tau pathology and likely precede neurodegeneration in Alzheimer's disease. *Acta Neuropathol* 118:475. <https://doi.org/10.1007/S00401-009-0556-6>
116. Sun W, Samimi H, Gamez M, Zare H, Frost B (2018) Pathogenic tau-induced piRNA depletion promotes neuronal death through transposable element dysregulation in neurodegenerative tauopathies. *Nat Neurosci* 21:1038–1048. <https://doi.org/10.1038/s41593-018-0194-1>
117. Tarkowski E, Issa R, Sjögren M, Wallin A, Blennow K, Tarkowski A et al (2002) Increased intrathecal levels of the angiogenic factors VEGF and TGF-β in Alzheimer's disease and vascular dementia. *Neurobiol Aging* 23:237–243. [https://doi.org/10.1016/S0197-4580\(01\)00285-8](https://doi.org/10.1016/S0197-4580(01)00285-8)
118. Taylor MS, LaCava J, Mita P, Molloy KR, Huang CRL, Li D et al (2013) Affinity proteomics reveals human host factors implicated in discrete stages of LINE-1 retrotransposition. *Cell* 155:1034–1048. <https://doi.org/10.1016/j.cell.2013.10.021>
119. Thomas CA, Tejwani L, Trujillo CA, Negraes PD, Herai RH, Mesci P et al (2017) Modeling of TREX1-dependent autoimmune disease using human stem cells highlights L1 accumulation as a source of neuroinflammation. *Cell Stem Cell* 21:319. <https://doi.org/10.1016/J.STEM.2017.07.009>
120. Tripathy D, Thirumangalakudi L, Grammas P (2007) Expression of macrophage inflammatory protein 1-α is elevated in Alzheimer's vessels and is regulated by oxidative stress. *J Alzheimer's Dis* 11:447–455. <https://doi.org/10.3233/JAD-2007-11405>
121. Tripathy D, Thirumangalakudi L, Grammas P (2010) RANTES upregulation in the Alzheimer's disease brain: a possible neuroprotective role. *Neurobiol Aging* 31:8. <https://doi.org/10.1016/J.NEUROBIOLAGING.2008.03.009>
122. Tsai AP, Dong C, Lin PB-C, Messenger EJ, Casali BT, Moutinho M et al (2022) *PLCG2* is associated with the inflammatory response and is induced by amyloid plaques in Alzheimer's disease. *Genome Med* 14:1–13. <https://doi.org/10.1186/S13073-022-01022-0>
123. Tuddenham JF, Taga M, Haage V, Roostaei T, White C, Lee A, Fujita M, Khairallah A, Green G, Hyman B, Frosch M, Hopp S, Beach TG, Corboy J, Habib N, Klein H-U, Soni RK, Teich AF, Hickman RA, Alcalay RN, Shneider N, Schneider J, Sims PA, Bennett DA, Olah M, Menon V, De Jager PL (2022) A cross-disease human microglial framework identifies disease-enriched subsets and tool compounds for microglial polarization. *bioRxiv*. <https://doi.org/10.1101/2022.06.04.494709>
124. Upton KR, Gerhardt DJ, Jesuadian JS, Richardson SR, Sánchez-Luque FJ, Bodea GO et al (2015) Ubiquitous L1 mosaicism in hippocampal neurons. *Cell* 161:228–239. <https://doi.org/10.1016/J.CELL.2015.03.026>
125. Vacinova G, Vejražkova D, Rusina R, Holmerová I, Vaňková H, Jarolímová E et al (2021) Regulated upon activation, normal T cell expressed and secreted (RANTES) levels in the peripheral blood of patients with Alzheimer's disease. *Neural Regen Res* 16:796. <https://doi.org/10.4103/1673-5374.295340>
126. Vonsattel JPG, del Amaya MP, Cortes EP, Mancevska K, Keller CE (2008) Twenty-first century brain banking: practical prerequisites and lessons from the past: the experience of New York Brain Bank, Taub Institute, Columbia University. *Cell Tissue Bank* 9:247–58. <https://doi.org/10.1007/s10561-008-9079-y>
127. Wang WY, Tan MS, Yu JT, Tan L (2015) Role of pro-inflammatory cytokines released from microglia in Alzheimer's disease. *Ann Transl Med* 3
128. Wang ZX, Wan Q, Xing A (2020) HLA in Alzheimer's disease: genetic association and possible pathogenic roles. *Neuromol Med* 22:464–473. <https://doi.org/10.1007/S12017-020-08612-4/FIGURES/2>
129. Wendeln AC, Degenhardt K, Kaurani L, Gertig M, Ulas T, Jain G et al (2018) Innate immune memory in the brain shapes neurological disease hallmarks. *Nature* 556:332–338. <https://doi.org/10.1038/s41586-018-0023-4>
130. Wightman DP, Jansen IE, Savage JE, Shadrin AA, Bahrami S, Holland D et al (2021) A genome-wide association study with 1,126,563 individuals identifies new risk loci for Alzheimer's disease. *Nat Gen* 53:1276–1282. <https://doi.org/10.1038/s41588-021-00921-z>
131. Wightman DP, Jansen IE, Savage JE, Shadrin AA, Bahrami S, Rongve A, Børte S, Winsvold BS, Drange OK, Martinsen AE, Skogholt AH, Willer C, Bråthen G, Bosnes I, Nielsen JB, Fritsche L, Thomas LF, Pedersen LM, Gabrielsen ME, Johnsen MB, Meisingset TW, Zhou W, Proitsi P, Hodges A, Dobson R, Velayudhan L, Team 23andMe Research, Sealock JM, Davis LK, Pedersen NL, Reynolds CA, Karlsson IK, Magnusson S, Stefansson H, Thordardottir S, Jonsson P V, Snaedal J, Zettergren A, Skoog I, Kern S, Waern M, Zetterberg H, Blennow K, Stordal E, Hveem K, Zwart J-A, Athanasiu L, Saltvedt I, Sando SB, Ulstein I, Djurovic S, Fladby T, Aarsland D, Selbæk G, Ripke S, Stefansson K, Andreassen OA, Posthuma D (2020) Largest GWAS ($N=1,126,563$) of Alzheimer's disease implicates microglia and immune cells. *medRxiv*. <https://doi.org/10.1101/2020.11.20.20235275>
132. Wylie A, Jones AE, D'Brot A, Lu WJ, Kurtz P, Moran JV et al (2016) p53 genes function to restrain mobile elements. *Genes Dev* 30:64–77. <https://doi.org/10.1101/gad.266098.115>
133. Xiao-Jie L, Hui-Ying X, Qi X, Jiang X, Shi-Jie M (2015) LINE-1 in cancer: multifaceted functions and potential clinical implications. *Genet Med* 18:431–439. <https://doi.org/10.1038/gim.2015.119>
134. Yin F (2023) Lipid metabolism and Alzheimer's disease: clinical evidence, mechanistic link and therapeutic promise. *FEBS J* 290:1420–1453. <https://doi.org/10.1111/FEBS.16344>
135. Yin Z, Raj D, Saiepour N, Van Dam D, Brouwer N, Holtman IR et al (2017) Immune hyperreactivity of Aβ plaque-associated microglia in Alzheimer's disease. *Neurobiol Aging*

- 55:115–122. <https://doi.org/10.1016/j.neurobiolaging.2017.03.021>
136. Zhou F, Sun Y, Xie X, Zhao Y (2023) Blood and CSF chemokines in Alzheimer's disease and mild cognitive impairment: a systematic review and meta-analysis. *Alzheimer's Res Therapy* 15:1–19. <https://doi.org/10.1186/S13195-023-01254-1>
137. Zhou Y, Song WM, Andhey PS, Swain A, Levy T, Miller KR et al (2020) Human and mouse single-nucleus transcriptomics reveal TREM2-dependent and TREM2-independent cellular responses in Alzheimer's disease. *Nat Med* 26:131–142. <https://doi.org/10.1038/s41591-019-0695-9>
138. Zhou Z, Liang Y, Zhang X, Xu J, Lin J, Zhang R et al (2020) Low-density lipoprotein cholesterol and Alzheimer's disease: a systematic review and meta-analysis. *Front Aging Neurosci* 12:503120. <https://doi.org/10.3389/FNAGI.2020.00005/BIBTEX>
139. (2023) 2023 Alzheimer's disease facts and figures. *Alzheimer's and Dementia* 19:1598–1695. <https://doi.org/10.1002/ALZ.13016>

Publisher's Note Springer Nature remains neutral with regard to jurisdictional claims in published maps and institutional affiliations.